Journal Pre-proofs

Investigating the prilling/vibration technique to produce gastric-directed drug delivery systems for misoprostol

Vita D'Amico, Nunzio Denora, Marianna Ivone, Rosa Maria Iacobazzi, Valentino Laquintana, Annalisa Cutrignelli, Massimo Franco, Michele Barone, Antonio Lopalco, Angela Assunta Lopedota

PII: S0378-5173(23)01184-5
DOI: https://doi.org/10.1016/j.ijpharm.2023.123762
Reference: IJP 123762

To appear in: *International Journal of Pharmaceutics*

Received Date: 13 November 2023
Revised Date: 29 December 2023
Accepted Date: 30 December 2023

Please cite this article as: V. D'Amico, N. Denora, M. Ivone, R. Maria Iacobazzi, V. Laquintana, A. Cutrignelli, M. Franco, M. Barone, A. Lopalco, A. Assunta Lopedota, Investigating the prilling/vibration technique to produce gastric-directed drug delivery systems for misoprostol, *International Journal of Pharmaceutics* (2024), doi: https://doi.org/10.1016/j.ijpharm.2023.123762

Investigating the prilling/vibration technique to produce gastric-directed drug delivery systems for misoprostol

Vita D'Amico [a], Nunzio Denora [a], Marianna Ivone [a], Rosa Maria Iacobazzi [a], Valentino Laquintana [a], Annalisa Cutrignelli [a], Massimo Franco [a], Michele Barone [b], Antonio Lopalco [a*], Angela Assunta Lopedota [a]

[a] *Department of Pharmacy-Pharmaceutical Sciences, University of Bari "Aldo Moro", Via E. Orabona, 4, I-70125 Bari, Italy*
[b] *Gastroenterology Unit, Department of Precision and Regenerative Medicine—Jonian Area—(DiMePRe-J), University of Bari "Aldo Moro", Policlinic University Hospital, Piazza G. Cesare 11, 70124 Bari, Italy*

*** Corresponding author:**
Department of Pharmacy – Pharmaceutical Sciences, University of Bari "Aldo Moro", Orabona St. 4, I-70125 Bari, Italy
E-mail addresses: antonio.lopalco@uniba.it

ABSTRACT

Prilling/vibration technique to produce oral microcapsules was explored to achieve local delivery of misoprostol (MIS), a prostaglandin E1 analogue indicated for the treatment of

gastric-duodenal ulcers, at the gastric mucosa. To improve MIS chemical stability and reduce its associated systemic side effects, drug delivery systems were designed and developed as microcapsules consisting of a core of sunflower oil and MIS (F_{s6} and F_{s14}) or a MIS complex with hydroxypropyl-beta-cyclodextrin (HP-β-CD) (F_{s18}), confirmed by specific studies, and a polymeric shell. The produced microcapsules showed high encapsulation efficiencies for those with MIS solubilized in sunflower oil (>59.86%) and for the microcapsules with MIS/HP-β-CD (97.61%). To demonstrate the ability of these systems to deliver MIS into the stomach, swelling and drug release experiments were also conducted in simulated gastric fluid. Among the three formulations, F_{S18} showed gastric release within 30 minutes and was the most advantageous formulation because the presence of the MIS/HP-β-CD inclusion complex ensured a greater ability to stabilise MIS in the simulated gastric environment. In addition, these new systems have a small size (<540 µm), and good flow properties and the dose of the drug could be easily adapted using different amounts of microcapsules (flexibility), making them a passepartout for different age population groups.

Keywords:
Misoprostol. Inclusion complex. Hydroxypropyl-beta-cyclodextrin. Prilling/vibration technique. Gastric-directed drug delivery systems.

1. Introduction

Misoprostol (MIS), a prostaglandin E1 (PGE1) analogue (Fig. 1) has potent antisecretory and cytoprotective effects on the gastric and duodenal mucosa (Garris and Kirkwood, 1989) and is indicated for the treatment of gastric-duodenal ulcers.

MIS inhibits acid secretion and can achieve its therapeutic effects locally in the stomach. Diarrhoea, stomach aches, and flatulence are associated with MIS systemic availability, though this is not a requirement for the protective antisecretory therapeutic effects. MIS side effects

could be reduced by site-specific release in the stomach. To obtain this goal approaches such as floating, swelling, and expandable systems, bioadhesive systems/mucoadhesive and high-density systems could be investigated (Adebisi and Conway, 2011). In these cases, the drug should be delivered to the stomach in a regulated, gradual manner, resulting in adequate local therapeutic levels while limiting systemic exposure and reducing the drug's adverse systemic effects.

Prostaglandins are difficult to formulate into stable pharmaceutical dosage forms because of their relative instability (Patel et al., 1973). MIS, like all E-type prostaglandins, is chemically unstable due to its susceptibility to pH and temperature factors. Indeed, under acidic or alkaline conditions, MIS can undergo dehydration and isomerization as well as a thermal epimerization reaction (Bellad and Goudar, 2006; Hagen et al., 2020). MIS is relatively stable when refrigerated but chemically unstable at room temperature (Collins et al., 1985), so, for oral therapy, a more stable dosage form at room temperature must be thought.

To address the stability issues of MIS some studies have found MIS to be more stable in a hydroxypropyl methylcellulose dispersion (Bimrew Sendekie Belay, 1990; Kararli et al., 1991). In addition, to obtain a local therapy that mitigates systemic impact, Oth and co-workers describe the development of floating capsules with a double layer. The first layer is designed to keep the dosage unit floating on the stomach contents while the second layer contains the drug formulated for sustained delivery (Oth et al., 1992). However, this study is dated, keeping in mind the enormous progress made by pharmaceutical technology in the last thirty years, such as the inclusion complex with cyclodextrins and the new technique of microencapsulation. Indeed, cyclodextrins can combine with PGE1 to form complexes that improve drug solubility and stability (Gu et al., 2005; Wlese et al., 1991) and changing the liquid MIS in a powder makes it easier to handle. Furthermore, several techniques, such as spray drying, fluidised bed coating, spray congealing, coagulation and prilling could be used for microencapsulation (Del Gaudio et al., 2009). The selection of the appropriate process depends mainly on the evaluation of several factors, including the physicochemical properties of the materials used and the size and structure of the final product. In particular, the prilling/vibration technique also known as a prilling or laminar jet breakup is a technique based on breaking a laminar jet of polymer solution into a line of mono-sized droplets using a vibrating nozzle device (D'Amico et al., 2023; Lopalco et al., 2020; Lopedota et al., 2021). The resulting droplets fall into a medium for consolidation and further collection. Prilling is a promising technology for the continuous production of large quantities of uniform spherical multiparticulate, both microspheres and microcapsules, with high encapsulation efficiency and excellent flow properties that can be sprinkled into suitable food (Khan et al., 2022) or swallowed directly by using a dose-measuring device, e.g., a measuring spoon or dose-sipping technology or successfully inserted into capsules (Breitkreutz and Boos, 2007).

Moreover, multiparticulates are flexible, easy to swallow and are acceptable for children after weaning (from about six months) although they may also be suitable for toddlers and infants if administered in a liquid vehicle (Walsh et al., 2011). Currently, oral indivisible tablets of MIS are on the market for the treatment of gastric-duodenal peptic-related diseases with strengths of 200 and 400 μg. These doses are appropriate for adults, but a concern arises when it is required a personalized dose, especially when the treatment with MIS is direct to children.

Starting from these considerations, this work aimed to investigate the prilling/vibration technique for the development of microcapsules loading MIS or its inclusion complex with hydroxypropyl-β-cyclodextrin (MIS/HP-β-CD), to obtain a flexible and personalised dosage form, easier to swallow, as an alternative to commercial tablets, and at the same time increasing the stability of MIS during storage conditions and in gastric fluids.

In detail, microcapsules, containing a core of MIS or MIS/HP-β-CD solubilized in vegetable oils or 1% w/v of Amprac 01, respectively, coated with a shell composed of selected polymeric pharmaceutical excipients (Fig. 1), were prepared using the prilling/vibration process. The

produced microcapsules were characterized in terms of drug loading, encapsulation efficiency, size, and morphology. To demonstrate the ability of these systems to deliver MIS into the stomach, drug release experiments were also conducted in simulated gastric fluid. Finally, studies were conducted to demonstrate the stability of MIS in these newly studied systems and its reduced degradation after administration in a gastric acid environment.

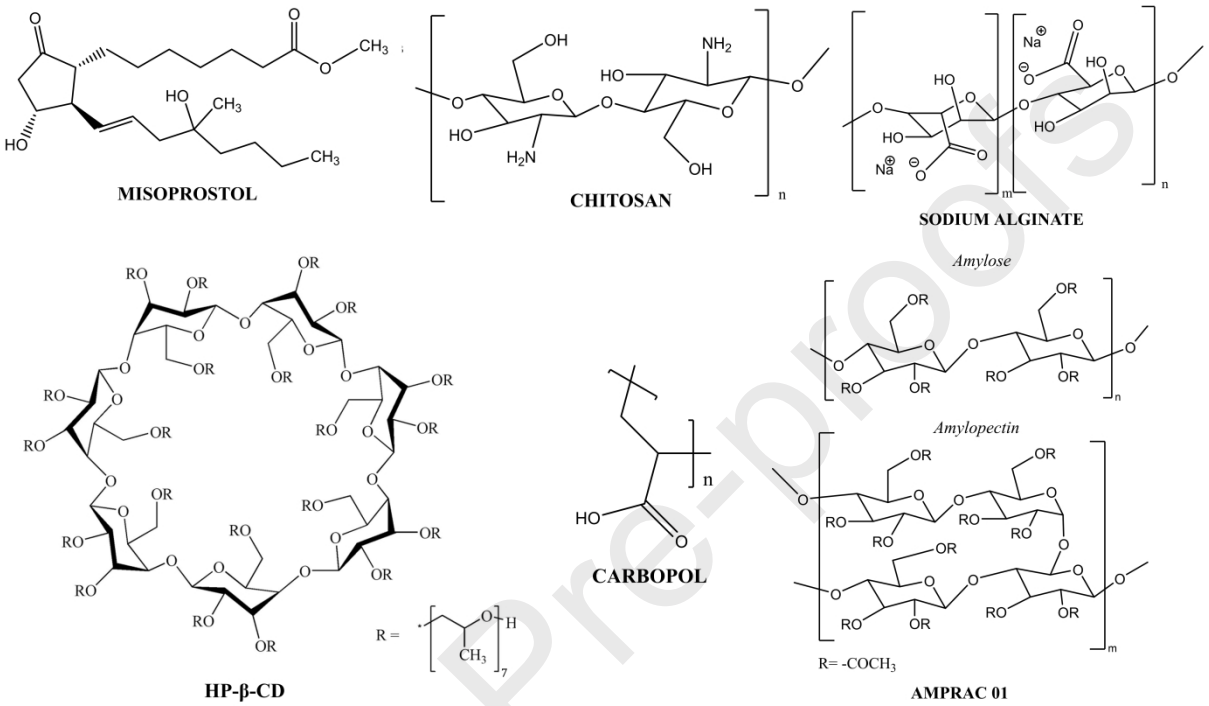

Fig. 1. Chemical structures of MIS, chitosan, sodium alginate, carbopol and Amprac 01.

2. Materials and methods

2.1 Materials

HP-β-CD (Cavasol W7, HP-β-CD with MW= 1540, molar substitution degree SD= 7), sodium alginate with a mannuronic acid to the guluronic acid ratio (M/G) of 1.8–2.2, Helianthus Annuus seed oil organic refined (density 0.9205 g/mL 25 °C), and extra virgin olea europaea oil (density= 0.920 g/mL at 25 °C) were obtained from Farmalabor Srl (Canosa di Puglia, Italy). Misoprostol (MW= 368.51), chitosan (low molecular weight MW= 50,000 - 190,000 Daltons), sodium triphosphate pentabasic, calcium chloride, and L-(+)-lactic acid were purchased from Sigma-Aldrich (Milan, Italy). Carbopol® 971P NF was purchased from Lubrizol (Bruxelles, Belgium). Amprac 01 was kindly donated by Evonik Nutrition & Care GmbH (Rofarma Italia Srl, Gaggiano, Italy). All solvents and other salts used were of analytical/technical grade and purchased from Sigma Aldrich.

2.2 High-Performance Liquid Chromatography (HPLC) analyses

Qualitative and quantitative analyses of MIS were carried out using a revised high-performance liquid chromatography (HPLC) method described in the literature (Kahsay et al., 2015). For the analysis, an Agilent Station was used consisting of a 1260 Infinity Quaternary LC System equipped with a variable wavelength UV detector, a Rheodyne injector (Rheodyne, Model

7725i) equipped with a 20 µL loop, and OpenLAB CDS ChemStation software (Agilent, Santa Clara, CA).

The HPLC method for quantifying MIS utilized a reversed-phase column, Zorbax SB-AQ (150 mm × 4.6 mm; 5 µm particles), as the stationary phase. The mobile phase consisted of a gradient mixture of mobile phase A (ACN–H_2O 30:70 v/v) and mobile phase B (ACN–H_2O, 50:50 v/v) pumped at a flow rate of 1.5 mL/min. The gradient programme [time (min)/%B] was set as 0/0, 5/0 to 15/35, 20/35 to 25/95, 30/95 to 32/0, 35/0. The spectrophotometric detector was operated at a wavelength of 200 nm and the column temperature of 35 °C was employed. The samples were quantified by measuring the areas of peaks, and the references were chromatographed under the same conditions. Agilent OpenLAB LC software was used for data analysis. MIS solutions with concentrations ranging from 1 mg/mL to 10 µg/mL were injected, and the peak areas were plotted against the corresponding concentrations to create a calibration curve described by a linear equation (y= 9472.711x, $R^2 > 0.9999$).

2.3 Phase solubility study and determination of inclusion complexation constant $K_{1:1}$

The phase solubility study of MIS with HP-β-CD was performed according to the Higuchi-Connors method (Higuchi T. and Connors K. A., 1965) with some modifications. A clearly visible excess of MIS was added in aqueous solutions of HP-β-CD (0-130 mM). The emulsion was sonicated and then allowed to settle for 1 h in a thermostatic bath at 25 °C ± 0.2 °C to allow separation of the excess MIS from the aqueous solution. The underlying solution was taken from the samples by removing the surface oil layer and, after appropriate dilution, the drug concentration was determined by HPLC according to the method described above. A solubility diagram was obtained by plotting the millimolar concentration of the drug against the HP-β-CD millimolar concentration. The following equation was applied to calculate the aqueous solubility and the inclusion constant of the drug with HP-β-CD ($K_{1:1}$):

$$K_{1:1} = \frac{p}{S_0 (1 - p)} \quad (12)$$

where:
S_0= Intrinsic solubility of MIS in water;
p= Slope of the phase solubility diagram.

In addition, the complexation efficiency (CE) and drug: cyclodextrin molar ratio (D:CD) was calculated using the Equation 2:

$$CE = \frac{slope}{(1 - slope)} \quad (2)$$

The drug-cyclodextrin molar ratio was calculated from the CE (Equation 3):

$$D{:}CD\ molar\ ratio = 1{:}\frac{(CE + 1)}{CE} \quad (3)$$

2.3.1 Inclusion complex stoichiometry determination (Job's plot method) by proton nuclear magnetic resonance spectroscopic (^{1}H-NMR) studies

The MIS/HP-β-CD inclusion complex in aqueous solution was analysed using the continuous variation method to verify stoichiometry. Briefly, equimolar (2 mM) D_2O solutions of MIS and HP-β-CD were mixed to a fixed volume by varying the molar ratio from 0 to 1, keeping the total molar concentration of the species constant. After stirring, for each solution, the proton nuclear magnetic resonance (^{1}H-NMR) spectra were registered, and the chemical shifts (δ) of the host's protons (H) were calculated and expressed as ppm. The variation of the chemical shift (Δppm) of the H of MIS was determined as the difference between δ of the hydrogen of the drug with and without HP-β-CD. Subsequently, Δppm × [MIS] was plotted versus r, where:

$$r = \frac{[MIS]}{[MIS] + [HP-\beta-CD]} \quad (4)$$

^{1}H-NMR spectra were carried out on Agilent VNMRS 500 MHz spectrometer, using D_2O as solvent. δ were referenced by using the residual solvent signal of D_2O at ~~4.79~~ 4.65 ppm.

2.3.2 Determination of complexation equilibrium constant $K_{1:1}$ by ^{1}H-NMR

A ^{1}H-NMR study was performed to determine $K_{1:1}$ for the molecular complex MIS/HP-β-CD as described in a previous work (Lopedota et al., 2015). Stock solutions in D_2O containing the compound of interest and HP-β-CD in a molar ratio of 1:20 respectively, were prepared and diluted with D_2O to cover a concentration range from 0.10 mM to 3.37 mM for MIS and from 2.11 mM to 67.47 mM for HP-β-CD. The ^{1}H-NMR spectra were recorded for the stock solutions and each of the five dilutions at 25 °C using D_2O as the internal standard. The units for δ of the H were mentioned as ppm. A difference in δ between complexed and MIS alone results from the shielding effects of HP-β-CD protons.
The Benesi-Hildebrand equation (Equation 5) was used for the determination of the complexation equilibrium constant $K_{1:1}$:

$$\Delta ppm_{obs} = \frac{\Delta ppm_{max} K_{1:1} [HP-\beta-CD]}{1 + K_{1:1}[HP-\beta-CD]} \quad (5)$$

where Δppm_{obs} corresponds to Δδ (observed difference in δ of examined hydrogens between complexed and free MIS), and Δppm_{max} corresponds to the hyperbolic asymptote of the curve.

2.4 Preparation and characterizations of MIS/HP-β-CD inclusion complex

The solid inclusion complex of MIS/HP-β-CD was prepared by lyophilisation. Briefly, the mixture of MIS and HP-β-CD was dissolved in water, and the resulting solution was rapidly frozen and lyophilised a Christ Alpha 1-4 LSC for 48 hours at reduced pressure (0.018 mbar) at -51 °C. The product once recovered was used immediately.
MIS/HP-β-CD inclusion complex was characterised in terms of both yield and drug content. For the drug content, a previously weighed aliquot of the MIS/HP-β-CD complex was solubilised in water and the MIS content was determined using the previously described HPLC method.
MIS/HP-β-CD inclusion complex was evaluated by InfraRed with Fourier Transformation (FT-IR) and electron microscopy technique (SEM) according to section 2.7.1. For FT-IR analysis, KBr pellets (2% of the sample) were analysed by a FT-IR 1600 Perkin Elmer spectrophotometer. Data were acquired between 4000 cm^{-1} and 400 cm^{-1}.

2.5 Preparation of feeds for the prilling/vibration technique

2.5.1 Feed without MIS

Initially, different polymer feeds were prepared for the formation of the final shell of the microcapsules.
For the shells, three feeds were considered as follows.

1) Two separate aqueous solutions of sodium alginate and carbopol at different concentrations (1.5% and 2% w/v) were prepared and mixed in different ratios adding 0.1% w/v titanium dioxide.
2) Chitosan aqueous solution was realised at different concentrations from 2% to 4% w/v using lactic acid (1% v/v) to promote solubilisation and finally 0.1% w/v titanium dioxide was added.
3) A solution of Amprac 01 at 8% w/v was obtained by stirring for 30 minutes gently in hot water (65 °C).

Sunflower oil, olive oil, aqueous solutions of 0.1% w/v alginate/carbopol [1:0.5], 0.1% w/v chitosan and Amprac 01 1% w/v were used for the inner core. The different feeds S_1-S_{18} were processed by prilling/vibration technique with an Encapsulator B395 Pro (Büchi, Switzerland) using different process parameters (Table 1) and according to the polymeric shell feed, different consolidation baths were tested (e.g., TPP, $CaCl_2$ and liquid nitrogen). When the process allowed the formation of hardened microcapsules, they were collected and immediately freeze-dried using a Christ Alpha 1-4 LSC for 48 hours at reduced pressure (0.018 mbar) at -51 °C.

Table 1. Polymer feeds (100 mL) and parameters used for the preparation of microcapsules using the prilling/vibration technique.

Feeds code	CORE	SHELL	Inner and outer nozzle size (µm)	Inner and outer flow rate (mL/min)	Frequency (Hz)	Electrode potential (V)
	Oil	***Alginate/ carbopol****				
S_1	Sunflower	1.5	450/ 600	2/ 19	1000	1500
S_2	Sunflower	1.33/ 0.667	300/ 600	1/ 16.5	800	1200
S_3	Olive	1.33/ 0.667	450/ 700	0.8/ 16	500	1000
S_4	Sunflower	1/ 1	300/ 600	1.5/ 19.5	1000	1500
S_5	Olive	1/ 1	450/ 700	1/ 20	1000	1200
S_6	Sunflower	1/ 0.5	300/ 500	0.8/ 18.8	600	1000
S_7	Olive	1/ 0.5	450/ 700	1/ 23.5	700	1100
	Alginate/ carbopol*	***Alginate/ carbopol****				
S_8	0.1	1/ 0.5	300/ 500	1/ 18.85	600	1000
	Oil	***Chitosan****				
S_9	Sunflower	4	300/ 700	-	-	-
S_{10}	Sunflower	3	300/ 600	1.2/ 8.2	600	1300
S_{11}	Olive	3	300/ 500	-	-	-
S_{12}	Sunflower	2.5	300/ 500	1.2/ 16	600	1000
S_{13}	Olive	2.5	300/ 400	-	-	-
S_{14}	Sunflower	2	300/ 500	1.2/ 15.25	600	1000
S_{15}	Olive	2	450/ 700	1.5/ 19.5	600	1000
	Chitosan*	***Chitosan****				
S_{16}	0.1	2	200/ 500	1.1/ 15.50	1000	1500
	Oil	***Amprac01****				
S_{17}	Olive	8	300/500	1/ 17.05	1000	1500
	Amprac01*	***Amprac01****				

S_{18}	1	8	200/ 300	1.5/ 11.33	1200	1500

*Expressed as g in 100 mL.

Then the most performing feeds S_6, S_8, S_{14} and S_{18} were selected to encapsulate MIS or MIS/HP-β-CD, in a concentration of 4 mg/mL of MIS, to obtain the different microcapsules F_{s6}, F_{s14} and F_{s18}, respectively (Table 2).

Table 2. Composition of microcapsules with MIS or MIS/HP-β-CD.

Formulations code	Core (g)	Shell (g)	MIS (mg)	MIS/HP-β-CD (g) *
F_{s6}	4.60 (sunflower oil)	1.76(alginate/carbopol)	20	-
F_{s8}	0.007(alginate/carbopol)	1.41(alginate/carbopol)	-	1.89
F_{s14}	4.60 (sunflower oil)	1.27 (chitosan)	20	-
F_{s16}	0.005 (chitosan)	1.41 (chitosan)	-	1.89
F_{s18}	0.05 (Amprac 01)	3.06 (Amprac 01)	-	1.89

* g of MIS/HP-β-CD inclusion complex carrying 20 mg MIS.

2.6 Characterization of the microcapsules

2.6.1 Production yield, encapsulation efficiency, and drug loading

The production yield percentage (Y%) for the process was determined using Equation (6~~4~~):

$$Y\,\% = \frac{\text{Mass obtained of microcapsules}}{\text{Total mass of feed components}} \times 100 \quad (6\text{~~4~~})$$

The encapsulation efficiency (EE) of MIS in microcapsules F_{s6} and F_{s14} was evaluated by disintegrating an exact amount of each formulation (600 mg) in 5 mL of methanol. Ultraturrax T 25 basic for 10 min at 13000 rpm was used to facilitate the complete disintegration of 100 mg of microcapsules F_{s18} and the dissolution of MIS in 3 mL of water. The final suspensions of each sample were centrifuged at 7500 rpm, 25 °C for 5 min, the supernatants were filtered with 0.22 µm cellulose acetate filters, and the concentration of MIS was determined by HPLC.
EE% and DL were computed using Equations (7 ~~5~~) and (8 ~~6~~), respectively:

$$EE\,\% = \frac{\text{Weight of MIS in microcapsules}}{\text{Weight of MIS added in the feed}} \times 100 \quad (7\text{~~5~~})$$

$$DL = \text{theoretical µg of MIS in 100 mg of microcapsules} \times EE\% \quad (8\text{~~6~~})$$

Analyses were conducted for each triplicate formulation and reported as mean ± standard deviation (SD).

2.7 Micromeritic studies

2.7.1 Microcapsules size, morphology, and inner structure

The sizes of the microcapsules were measured by optical microscopy (Inverted Laboratory Microscope Optech IB 4) equipped and interfaced with an image analysis program (Capture 2.1 software).

The morphology of the selected microcapsules (F_{s6}, F_{s14} and F_{s18}) and the inclusion complex MIS/HP-β-CD was determined by scanning electron microscopy (SEM) using a Hitachi Tabletop Microscope TM300 and a secondary electron detector SED high vacuum mode, acceleration voltage 20 kV and EI Magnification 60×–1000× and interfaced with an analysis program (AZtecOne software). The microcapsules or their pieces were sprinkled on an adhesive pad with electrical conductivity before being covered in a gold/palladium layer (sputter coating, 15–20 nm).

2.7.2 Determination of flow properties

The flow characteristics of the microcapsules (F_{s6}, F_{s14} and F_{s18}) were evaluated by determining the angle of repose. The indirect or static approach was used to evaluate the angle of repose using an instrument (Flowability tester BEP2) designed to assess a powder's ability to flow through an aperture. After the known quantity of material was funnelled through, the height of the cone (h) formed on a surface with a circular base and a known radius (r) of 2.5 cm was measured. The angle of repose (°), defined as the angle between a dust cone's free surface and a horizontal plane, was calculated using Eqs. (9~~7~~) and (10~~8~~):

$$\text{tang}\,\alpha^\circ = \frac{h}{r} \quad (9\text{~~7~~})$$

$$\alpha^\circ = \text{arctang}\,\alpha^\circ \quad (10\text{~~8~~})$$

The bulk and tapped densities were measured using the JV1000 series volumetric crusher (Copley) and the test described in the Italian Pharmacopoeia (Ist. Poligrafo dello Stato, 2008). A weighed quantity of microcapsules (10 g) was introduced into a graduated cylinder of 100 mL capacity.

The bulk density (ρb) was calculated by dividing the mass of the microcapsules by the bulk volume. With a constant height of 3 ± 0.2 mm and a pace of 250 taps per minute, the cylinder was tapped for one minute. This was done to determine the tapped volume and density (ρt). The t is calculated from the measurement made after the sample was mechanically crushed.

Equations were used to calculate the Carr's index (Eq. 11 ~~9~~) and Hausner ratio (Eq. 12~~10~~):

$$\text{Carr's index} = \frac{\rho t - \rho b}{\rho t} \times 100 \quad (11\text{~~9~~})$$

$$\text{Hausner ratio} = \frac{\rho t}{\rho b} \quad (12\text{~~10~~})$$

2.7.3 Swelling behaviour

The gravimetric method was used to evaluate the dried microcapsules' swelling behaviour. Microcapsules that had previously been weighed were put inside a cylinder with a known tare and a square mesh base. The swelling experiments were carried out at a temperature of 37 ± 0.5 °C, dipping the cylinder in the fluid simulating the gastric-enteric environment (pH 1.2 for 2 h and then pH 6.8 until the end of the experiment for F_{s6} and F_{s14} and only pH 1.2 for 2 h for F_{s18} due to their complete degradation).

The cylinder containing the sample was weighed and lightly dried with paper at predetermined intervals. The swelling (Sw%) of the microcapsules with respect to time was calculated according to the Eq. ~~11~~13:

$$Sw(\%) = \frac{Wf - Wi}{Wi} \times 100 \quad (13~~11~~)$$

where W_f is the weight of the microcapsules after being rehydrated in the simulated gastroenteric fluids and W_i is the initial weight of the microcapsules.

2.8 Drug release studies

Release studies were conducted using a VanKel VK 7000 with the paddle rotating at 50 rpm and the temperature of the dissolution medium was maintained at 37 ± 0.5 °C. Release studies of MIS from the F_{s6}, F_{s14} and F_{s18} formulations were carried out by points using gastric pH medium (HCl 0.1 M, pH= 1.2) for 2 h. F_{s6}, F_{s14} and F_{s18} microcapsules were placed in different vessels, each with 100 mL of medium to obtain a final MIS concentration of 50 µg/mL. At specific times (0, 2, 5, 15, 30, 45 and 70 min), samples with a volume of 500 µL were taken from a vessel. The samples were centrifuged (at 7500 rpm, 25°C for 5 min) and the supernatants were analysed by HPLC to determine the percentage of cumulative MIS release. The microcapsules were taken, and disintegrated by the method described above and the concentration of MIS still present in the microcapsules was measured by HPLC analysis.

2.9 MIS Degradation Kinetic Study in Simulated Gastric Environment

The study of MIS degradation kinetic was performed to assess its chemical stability in the gastric environment with or without cyclodextrin. In detail, MIS or MIS/HP-β-CD inclusion complex was placed in the simulated gastric medium at pH 1.2 and at 37°C to obtain a final concentration of MIS equal to 1 mg/mL, and at certain time points, samples were taken and analysed by HPLC to evaluate changes in drug concentration versus time.
The data obtained were fitted using three mathematical models including a zero-order model (degradation reactions do not depend on the concentration of the drug and stress), a first-order model (degradation reaction rate is proportional to the decrease in initial drug concentration as a function of time), second-order model (when the rate is proportional to the square of the concentration of the drug) (Bhangare et al., 2022).

2.10 Physical Stability of Microcapsules and Chemical Stability of MIS in the Formulations

The physical stability of F_{s6}, F_{s14} and F_{s18} was assessed by visual inspection to evaluate possible changes in colour, diameter, and presence of oil on the surface, and the chemical stability of MIS in the three formulations was performed by HPLC analysis. The samples were stored in closed amber vials in a Thermofisher refrigerated orbital shaker at room temperature (25 ± 0.5 °C), in the fridge (4 ± 0.5 °C), and in a climatic chamber (40 ± 0.5 °C and 60% of RH) (Climacell 222 – ECO line, MMM Group, Semmelweis Strasse, München, Germany). Analyses were carried out at time 0 and 2 months.

2.11 Statistical analysis

The experimental data are reported as the mean ± SD (standard deviation). Statistical analyses were conducted using Graph Prism version 8.0.1 (GraphPad Software Inc., La Jolla, CA, USA). When comparing data sets for statistical significance, one-way ANOVA analysis, followed by Bonferroni's post hoc tests was performed, adhering to a p value of <0.0001. Statistically differences are reported as follow: ns = p value >0.05; *= p <0.0332; **= p value <0.0021; ***= p value <0.0002; **** = p value <0.0001.

3 Results and discussion

The prilling/vibration technique was investigated for the development of an oral formulation for gastric delivery of MIS. This technique was used to design and develop drug delivery systems such as microcapsules, which are easily swallowable and flexible in dosage. As the great importance of using cyclodextrins both as solubilising and stabilising agents is well known, in this study, we also evaluated the possibility of producing an inclusion complex between MIS and HP-β-CD to improve the chemical stability of MIS and reduce the associated systemic side effects.

3.1 Phase solubility study and determination of inclusion complexation constant $K_{1:1}$

As the application of cyclodextrins as complexing agents to increase the aqueous solubility of poorly soluble drugs, to increase their bioavailability and improve their stability is well known (Saokham et al., 2018; Tiwari et al., 2010), in this work we focused on the use of HP-β-CD, which monography is available in the Ph. Eur. and is cited in the FDA's list of Inactive Pharmaceutical Ingredients. HP-β-CD is the most studied cyclodextrin due to its high-water solubility (> 300 mg/mL) compared its parent β-CD (18.5 mg/mL), its low toxicity compared to other semisynthetic cyclodextrins, such as the randomly methylated β-CD (Brewster and Loftsson, 2007), and its high complexation profile (D'Aria et al., 2022; Gould and Scott, 2005).
The phase solubility study was performed for a short time due to the instability of MIS, to assess (Monkhouse et al., 1973) the effect of cyclodextrin complexation on the solubility of the drug in water (MIS aqueous solubility (S_0) equal to 3.38 mM; 1.29 mg/mL).
The phase solubility diagram shows a significant and linear increase in MIS aqueous solubility in the presence of increasing HP-β-CD concentrations (Fig. 2A). The regression analysis (R^2= 0.9919) describes an AL-type curve, according to the Higuchi-Connors classification, with a slope p equal to 0.4868, which is associated with the formation of a complex with a 1:1 stoichiometry between MIS and HP-β-CD. Using the Higuchi-Connors equation, the experimental complexation constant ($K_{1:1}$) was equal to 280.86 ± 7.48 M^{-1}. However, the determination of complex association constants K by titration method such as ^{1}H-NMR holds greater relevance than the one based on solubility diagrams, as described by Loftsson (Loftsson et al., 2005). Therefore, further studies by ^{1}H-NMR have been conducted for the determination of the inclusion complexation constant. ~~This value agrees with the values described in the literature (Gu et al., 2005) for the investigation of the effect on the aqueous solubility and stability of PGE_1 and analogues in the presence of different cyclodextrins. Moreover, the value obtained indicates a good interaction between MIS and HP-β-CD. In fact, complexation constants between 50 and 2000 M^{-1} are considered advantageous (Loftsson et al., 2005; Mahmood et al., 2015).~~ The CE value is an important aspect to consider when evaluating the solubilising efficiency (Lopalco et al., 2022). The CE value is 0.9486 and the ratio of drug to HP-β-CD is 1 to 2.
~~We confirmed the stoichiometry of the inclusion complex by using the continuous variation approach, commonly known as the Job's diagram method. In detail, this study was conducted via ^{1}H-NMR by observing the variation of chemical shifts of methyl hydrogens (CH_3) on the aliphatic chain and the protons of the cycle (CH_2) of MIS. Based on the chemical shift of the~~

~~CH_3 protons on the aliphatic chain of MIS, Job's graph was created. Therefore, this methyl group is directly involved in complexation with cyclodextrin. As shown in Fig. 2b, a very symmetrical trend is observed throughout the considered range, with a maximum value recorded at r= 0.5, confirming the creation of a 1:1 inclusion complex observed in the phase solubility study.~~

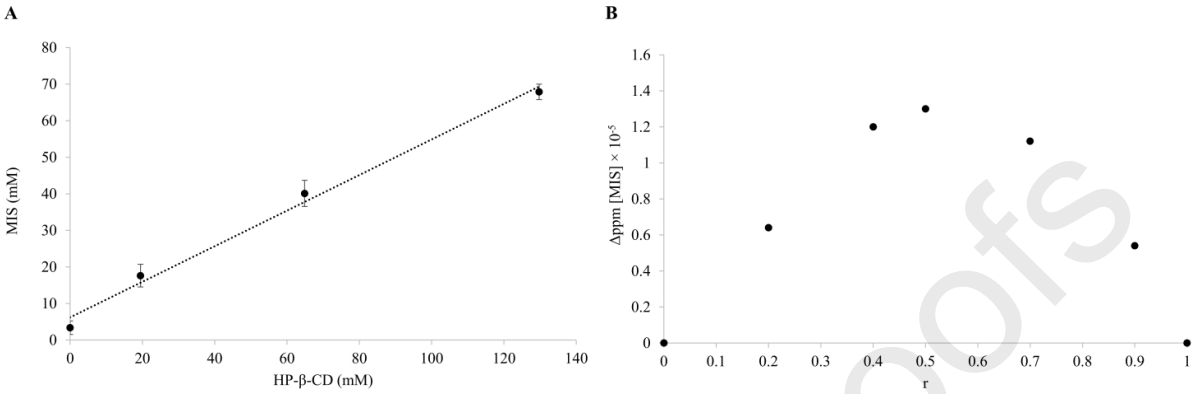

Fig. 2. (A) Phase solubility studies of MIS/HP-β-CD complex. (B) A representative Job's plot diagram for the determination of MIS/HP-β-CD stoichiometry was obtained by plotting the Δppm of the hydrogen of MIS on the C in position 12 versus r.

3.2 Inclusion complexation constant $K_{1:1}$ and stoichiometry (Job's plot method) determination by ^{1}H-NMR studies

Fig. 3 shows ^{1}H-NMR spectra of HP-β-CD (A), the pure MIS (G), and the five dilutions of a mixture of the two stock solutions (B-F). From the spectra analyses, we could observe a change in δ of the several H of MIS, of the two chains and the oxo-cyclopentyl ring. The most significant changes of δ were observed on the hydrogens of the ring (positions 11 and 12) and those on the C of alkene (positions 14 and 15). We could not investigate the shift of all the signals of MIS since many of them were overlapped by the signals of the HP-β-CD. As one can see from the spectra, by evaluating different δ of the hydrogens of the C in positions 11, 12, 14 and 15, their signals shift downwards (to higher ppm) as the concentration of HP-β-CD increases (Table S1). This can be justified by the increasing of the fraction of MIS complexed with cyclodextrin.
The mean value of the $K_{1:1}$ obtained from the curve fitting analysis of these hydrogens is 1080.89 M^{-1}, a value in agreement with that reported in the literature by Gu and co-workers for the complexation of a PGE1 with HP-β-CD (Gu et al., 2005). This $K_{1:1}$ value compared to the complexation constant obtained from the phase solubility diagram indicates that the determination of $K_{1:1}$ by the ^{1}H-NMR titration method is more accurate and precise than the value obtained by solubility diagrams. In fact, the Benesi-Hildebrand equation avoids using the solubility of the drug by overcoming the uncertainty of the phase solubility study.

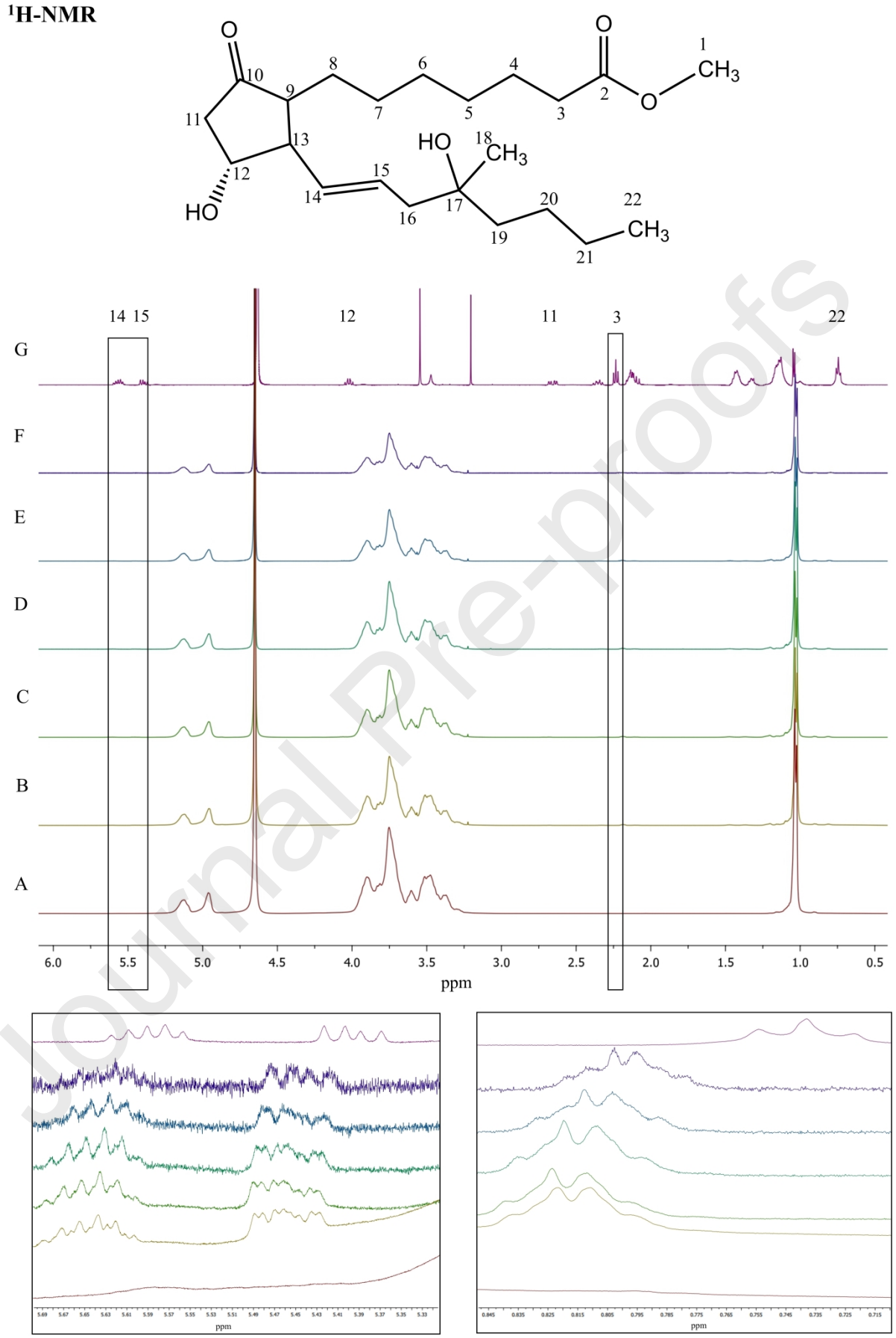

Fig. 3. NMR spectra of HP-β-CD at a concentration of 67.47 mM (A), MIS at a concentration of 3.372 mM (G), and the five dilutions of a mixture of the two stock solutions (B-F). The insets

present a zoom of the region in the black frames to highlight the changes in the δ of the H signals on the C in positions 3, 14 and 15 of MIS with an increase of HP-β-CD concentration.

The stoichiometry of the inclusion complex was evaluated following the observable δ of hydrogens on the C in positions 11, 12, 14, 15 and 22. As shown in Fig. 2B and in Fig. S1A-E in Supplementary Information very symmetrical trends are observed throughout the considered range, with maximum values recorded at r equal to 0.5, confirming the stoichiometry of the complexation of 1:1.

3.3 Preparation and characterizations of the MIS/HP-β-CD inclusion complex

The manufactured MIS/HP-β-CD complex is presented as a homogeneous, high-quality powder product. The values in terms of yield following the freeze-drying process were found to be 99.60 ± 0.37% while the complexed drug content was evaluated by HPLC analysis and the EE% was found to be 97.84 ± 0.63%. The high efficiency demonstrated that the selected method of complexing provided excellent host-guest interaction conditions (Santos et al., 2015).
The formation of the inclusion complex was verified by solid-state characterisation studies using FT-IR analysis (Fig. ~~3~~ 4), and it was observed that peaks around 3300 cm^{-1} were characteristic of HP-β-CD. In the bands at 3500–3200 cm^{-1}, there is an axial deformation of the associates O–H. In the 2940-2850 cm^{-1} region, an axial deformation of the aliphatic C-H bond occurs. The peak at 1449 cm^{-1} can be attributed to an angular deformation of CH_2 adjacent to the carbonyl. In the region between 1180-1030 cm^{-1}, C-O angular deformation of the ethers is observed. The MIS peaks at 2522 and 2594 cm^{-1} in the FT-IR spectrum of MIS/HP-β-CD disappear and this could be a sign of interaction between the drug and cyclodextrin with the probable formation of a solid-state inclusion complex.

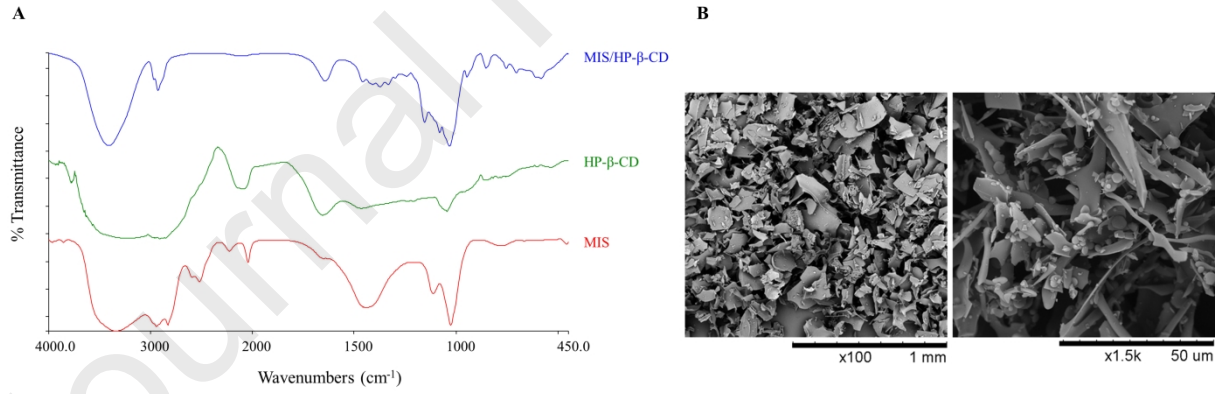

Fig. ~~3~~ 4. FT-IR spectra ~~and thermograms~~ (A) and SEM images of the inclusion complex MIS/HP-β-CD (B).

SEM images (Fig. 3B) show the morphology of the MIS/HP-β-CD inclusion complex, which appears with a disorganised structure following the lyophilisation process.

3.4 Production of microcapsules

The first part of the study focused on the choice of polymers and the identification of the best feed composition to make microcapsules for gastric delivery.
The idea was to produce microcapsules with mucoadhesive, and possibly floating characteristics based on biocompatible and/or biodegradable polymers able to guarantee the release of MIS within a short period of time. Several polymeric excipients, polysaccharides of natural origin with different characteristics, were selected to produce the shell. Sodium alginate is a versatile polymer, widely used in the production of dosing systems for oral applications, due to its

biocompatibility and mucoadhesive capacity (Jadach et al., 2022; Russo et al., 2016). It is used to produce gastric-release drug delivery systems as it can produce swellable and floating formulations that can gradually release the drug at the desired rate (Sen et al., 2023). Carbopol has good biodegradable and mucoadhesive properties (Bera et al., 2016), as does chitosan. Chitosan is a bioadhesive, non-toxic biopolymer capable of forming floating, mucoadhesive drug systems that can establish various types of interactions with the gastric mucosa and is used in the development of gastroretentive drug delivery systems (Souza et al., 2020). Amprac 01 is a pregelatinised maize starch used as a film-forming polymer (Bonacucina et al., 2006), characterised by high safety, renewability, and biodegradability. In this work, its use to make swellable microcapsules with controlled release was investigated. Pregelatinisation of starch causes increased swelling power, which induces rapid disintegration and faster release in an acidic environment (Zheng et al., 2023). Furthermore, pregelatinised starches also tend to improve the solubility of poorly soluble drugs by increasing their dissolution (Kankate et al., 2020).

MIS appears as an oil, chemically unstable in water (Berard et al., 2014; Bizimana et al., 2021), and therefore an appropriate oil vehicle was used as a core. In contrast, the MIS/HP-β-CD inclusion complex was solubilized in an aqueous-based core due to its increased chemical stability in water, as shown in section 3.9 ~~by stability studies~~. The oils chosen were olive and sunflower seed oil characterised by numerous antioxidant and anti-inflammatory properties (Odabasoglu et al., 2008). In fact, their intake is recommended in cases of gastritis because they stimulate the production of mucin, which can protect the stomach walls.

Following the selection of the shell constituents, several preliminary tests were performed to determine the most appropriate consolidation baths for each feed and the most suitable for producing the microcapsules. For example, the optimal concentration of pentabasic sodium triphosphate (TPP) and $CaCl_2$ was studied. Chitosan, being a positively charged polymer, can cross-link through ionic gelatinisation with TPP, which was used at a concentration of 4% w/v, as it allowed for adequate consolidation of the microcapsules without them sticking together. 0.3M $CaCl_2$ was used as an appropriate gelling agent, as it induces ionotropic gelation of the alginate/carbopol droplets. In the case of Amprac 01, a nitrogen consolidation bath was used, employing the prilling/congealing technique, which allows immediate freezing after falling into liquid nitrogen.

Table 3 shows the pre-formulation systemic study that was followed to select the most suitable polymeric feeds to produce microcapsules, initially without drug, with suitable characteristics for the formulation purposes set (high yields, limpid consolidation bath, spherical particles, with homogeneous diameters in a narrow size range and not oily to the touch).

Once the polymeric feed was prepared, the first selection step was the processability of the latter. As shown in Table 3, the processability of the different feeds was influenced by the concentrations and viscosities, as they could affect specified characteristics of the final product such as, for example, the particle size. Indeed, the lower the viscosity of the starting material, the smaller the diameter of the microcapsules obtained is likely to be (Uyen et al., 2020). For example, the S_9 and S_{13} feeds were not suitable for processing due to the high concentration of chitosan (4% w/v) clogging the nozzle, and the core nozzle diameter being unsuitable for processing olive oil respectively and were therefore discarded for further study. The S_3, S_5 and S_{11} feeds, although processable, lost a lot of olive oil in the consolidation bath, producing partially empty, inhomogeneous, and oily microcapsules on the surface. The S_{10} feed produced microcapsules that were non-uniform both in size and in the distribution of the encapsulated oil, highlighting the incorrect choice of the nozzle diameters selected. The S_1 feed produced aggregate microcapsules with very low yields (<46%) due to oil loss in the bath. The S_2 and S_4 feeds were also rejected due to yields of less than 86%, which was the limit imposed for the selection of the best-performing microcapsules. S_7 and S_{15} despite discrete yields (79.96% and 68.75% respectively) compared to the previous feeds, produced non-spherical and oily

microcapsules on the surface after the freeze-drying process, leading us to discard these as well. The S_{12} feed, while having yields within the limits required by our studies (86.93%), produced microcapsules with a diameter above the required standard, i.e., 1.3 mm. The S_{17} feed, in which the core consisted of oil, yielded high yields but produced microcapsules in which the core was unevenly distributed, non-spherical, inhomogeneous, partially hollow with larger diameters than those produced by the S_{18} feed in which the core consisted of a 1% w/v aqueous solution of Amprac 01, which demonstrated easier processability (microcapsules coded as F_{s18}). In addition, the microcapsules obtained from the S_{18} feed with an Amprac 01 shell also showed favourable characteristics in terms of homogeneity, sphericity, high yields, and smaller diameters than the corresponding F_{s17} microcapsules, which, however, have an oil core. S_6, S_8, S_{14} and S_{16} also satisfied our needs, producing microspheres with high yields, homogeneous dimensions and neither sticky nor collapsed. Consequently, we selected five formulations (F_{s6}, F_{s8}, F_{s14}, F_{s16} and F_{s18}) from our initial study, which were considered suitable to be loaded with the drug and investigated further.

Table 3. Selection of empty microcapsules, based on polymer feed processability, yield and diameter range.

Feeds code	Processability of feeds	Microencapsulation	Yield (%)	Diameter (µm)	Formulations code
S_1	Yes	Yes	45.86 ± 10.03	957.02 ± 103.95	-
S_2	Yes	Yes	60.04 ± 15.96	893.67 ± 124.81	-
S_3	Yes	No	-	-	-
S_4	Yes	Yes	73.95 ± 12.67	906.82 ± 105.03	-
S_5	Yes	No	-	-	-
S_6	Yes	Yes	87.46 ± 9.84	884.25 ± 30.71	F_{s6}
S_7	Yes	Yes	79.96 ± 12.15	1349.69 ± 147.18	-
S_8	Yes	Yes	89.57 ± 3.08	847.59 ± 18.09	F_{s8}
S_9	No	No	-	-	-
S_{10}	Yes	No	-	-	-
S_{11}	No	No	-	-	-
S_{12}	Yes	Yes	86.93 ± 8.06	1753.14 ± 87.24	-
S_{13}	No	No	-	-	-
S_{14}	Yes	Yes	92.36 ± 7.05	1238.01 ± 46.03	F_{s14}
S_{15}	Yes	Yes	68.75 ± 13.09	1711.15 ± 271.95	-
S_{16}	Yes	Yes	91.50 ± 4.80	904.06 ± 20.48	F_{s16}
S_{17}	Yes	Yes	89.65 ± 4.35	893.74 ± 172.82	-
S_{18}	Yes	Yes	99.53 ± 3.62	541.46 ± 30.16	F_{s18}

3.5 Production yield, EE%, and DL

The best empty formulations (F_{s6}, F_{s8}, F_{s14}, F_{s16} and F_{s18}) obtained by the prilling/vibration technique were loaded with the drug. MIS is an oil and, to be processed by the prilling/vibration technique, it must be diluted with a suitable lipophilic vehicle. MIS as such was loaded in a sunflower oil core (F_{s6}, F_{s14} ~~and F_{s17}~~), due to its instability in an aqueous environment (Collins et al., 1985; Gu et al., 2005) or as MIS/HP-β-CD inclusion complex solubilized in a core consisting of a 1% w/v aqueous solution of Amprac 01 (F_{s8}, F_{s16}, F_{s18}).

An excess of cyclodextrin was used to confer consistency to the aqueous core, have a cryoprotective effect on the microcapsules and protect during the lyophilisation process (Vega et al., 2012; Zaghloul et al., 2022).

The EE%, drug loading and production yield of the prepared microcapsules loading MIS or its inclusion complex are shown in Table 4. According to this table, the production yield of the obtained microcapsules confirmed the success of the adopted process. What can be highlighted is the difference in yield between the F_{s8} and F_{s16} formulations empty and loaded with the MIS/HP-β-CD inclusion complex. In fact, the yield values of the two empty formulations were 89.57% and 91.50%, while those of the loaded formulations were 34.71% and 46.06% for F_{s8} and F_{s16} respectively. This reduction is probably due to the higher aqueous solubility of MIS/HP-β-CD in the consolidation bath, where it can easily escape ~~to~~ from the polymer matrix still present in a transient semi-solid state (Jyothi et al., 2010) and diffuse into the aqueous bath. This results not only in a massive weight loss of the microcapsules with consequent yield reduction but also in a reduction of the EE%, as the MIS is complexed in the HP-β-CD and is lost in the consolidation bath (D'Amico et al., 2023). Considering these results, these two formulations (F_{s8} and F_{s16}) were discarded and not characterised by further studies.

The yield percentage for the other formulations (F_{s6}, F_{s14} and F_{s18}) was very high (87.46%, 92.36% and 99.53%). The F_{s6} formulation shows a slightly lower yield than F_{s14}, probably due to the lower cross-linking capacity of the alginate/carbopol mixture compared to chitosan, which leads to the formation of a less dense and compact shell. Indeed, like the yield, the lower EE% is due to the loss of the core oil vehicle and thus a partial loss of MIS during prilling in the crosslinking bath and during the freeze-drying process. The F_{s18} formulations showed high EE% values (97.61%), as did the yield. These results are due to the possibility of processing MIS not as oil but as a powder inclusion complex solubilized in the aqueous polymeric feed of the core, facilitating processability and improving the chemical stability of the drug. Furthermore, no losses occurred due to the consolidation method used. To our knowledge, the prilling/congealing technique (Lopalco et al., 2020), which ensures immediate freezing of the feed when dropped into liquid nitrogen, has not been used in previously published studies with Amprac 01.

DL values for the tested formulations ranged from 65.00 to 280.49 µg MIS per 100 mg microcapsules. These values doubled or halved the amount of MIS loaded, respectively, as the EE values remained the same (data not shown). These values suggest that the microcapsules made are both flexible dosage formulations and units capable of different loading strengths.

Table 4. Yield%, EE%, DL, and size of the dried microcapsules loading MIS or MIS/HP-β-CD. Data are reported as the mean ± SD.

Formulation Code	Yield%	EE%	DL*	Diameter microcapsules (µm)
F_{s6}	87.46 ± 9.84	59.86 ± 2.85	102.04 ± 8.90	879.01 ± 43.16
F_{s8}	65.82 ± 3.16	38.62 ± 2.69	65.00 ± 1.28	892.84 ± 46.91
F_{s14}	92.36 ± 7.05	69.99 ± 3.13	124.59 ± 2.24	1250.39 ± 61.44
F_{s16}	46.06 ± 2.04	43.80 ± 4.49	65.24 ± 2.05	926.63 ± 17.49
F_{s18}	99.53 ± 3.62	97.61 ± 2.15	280.49 ± 1.37	537.28 ± 26.07

* DL is expressed as µg of MIS per 100 mg of microcapsules.

3.6 Micromeritic studies of microcapsules

Dimensional studies were carried out to evaluate the microcapsules' average diameter and assess whether the diameter of the formulations made was smaller than the maximum diameter of 1.3 mm that we had set as an acceptable limit. These dimensional values are critical to make the formulations acceptable to the patient (Lopez et al., 2015). The mean diameters of the dried microcapsules are shown in Table 4. The size of these microcapsules varies considerably depending on the feed used to make the shell. The use of chitosan produced larger microcapsules than those of alginate/carbopol, despite the fact that the same nozzles were used, probably due to the different flow rates and the greater adhesion of the food to the nozzle edge, resulting in larger droplets forming at the nozzle exit before detachment due to vibration (Del Gaudio et al., 2005). As can be seen by comparing the diameters of the empty formulations (Table 3) and the same formulations loaded with the drug (Table 4), they are very similar, underlining the validity of the process used and that the MIS or its inclusion complex does not in any way affect the processability and diameters of the microcapsules produced. Although all three formulations have a smaller diameter than that identified as the limit, F_{s18} is smaller than all other microcapsules, with an average diameter of 537.28 µm. This reduction in the diameter of the microcapsules is associated both with a reduction in the nozzles used (200 and 300 µm) and with easier processability of the feed. In fact, the absence of an oily phase in the core considerably reduced the adhesive forces at the nozzle level, allowing the droplets to be detached more easily and quickly, thus making them smaller. The microcapsules' diameters realised, especially the F_{s18}, are acceptable considering a multiparticulate formulation that is flexible in dosage and easily taken by any age group of patients, including children.

The microcapsules produced could be packaged in single or multiple dosage forms ~~shapes~~; therefore, it is important to assess the flow properties to be able to distribute the microcapsules evenly by weight (Soppimath et al., 2001). The results obtained from the F_{s6}, F_{s14}, and F_{s18} microcapsules are shown in Table 5. All the formulations analysed were free flowing, as indicated by the angle of repose value of less than 25°. Carr's index and Hausner ratio are indirect values of bulk density and inter-particle friction or material cohesion, which depend on several properties, including material type, particle shape, size, surface area, and particle forces (e.g., electrostatic cohesion) (Rough et al., 2003). Hausner's ratio ranged from 1.04 to 1.16, showing in accordance with the Slip Attitude Scale (Ist. Poligrafo dello Stato, 2008) an excellent flux for F_{s14} and F_{s18} and a good flux for F_{s6} probably due to the slightly more irregular shape, rougher surface, and slightly stickier surface of these microcapsules than the others, which increase inter-particle friction (Abdullah and Geldart, 1999). Carr's index ranged from 3.96 (F_{s18}) to 14.10 (F_{s6}), again indicating excellent (for F_{s18} and F_{s14}), and good (for F_{s6}) compressibility and the absence of cohesive forces. These results suggest that all formulations have good flow characteristics and are suitable for easy packing with high flexibility.

Table 5. Bulk density, tapped density, Carr index, Hausner ratio, and angle of repose. Data are reported as the mean of results ± SD.

Formulation code	Bulk density (g/mL)	Tapped density (g/mL)	Carr index	Hausner ratio	Angle of repose (°)
F_{s6}	0.2162 ± 0.02	0.2517 ± 0.03	14.10 ± 0.01	1.16 ± 0.02	25.37 ± 0.59
F_{s14}	0.1444 ± 0.07	0.1565 ± 0.05	7.73 ± 0.04	1.08 ± 0.04	18.00 ± 0.41
F_{s18}	0.0533 ± 0.03	0.0555 ± 0.03	3.96 ± 0.03	1.04 ± 0.02	21.40 ± 0.38

Fig.-4 5A-D shows SEM images of the lyophilized microcapsules. The F_{s6} microcapsules appear non-spherical, with jagged edges. The surface details (Fig.-4 5B) show the presence of oil droplets, numerous cavities, and pores. Most probably, the loss of water occurring during freeze-drying resulted in the formation of irregular, porous structures with an extensive network of

wrinkles due to the breakdown of the shell in which the alginate was cross-linked with calcium (Aquino et al., 2012). The cross-section images of the microcapsules were difficult to obtain due to the high oiliness (Fig. 4- 5C,D). In contrast, the F_{s14} microcapsules are more spherical, with regular margins, a homogeneous but folded surface, and no trace of oil is visible on the surface (Fig. 4B). The cross-section shows a typical polynucleate structure and from the detail (Fig. 4-5C) the presence of oil inside the microcapsules can be seen. The morphology of the F_{s18} microcapsules appears completely different from that of all the other microcapsules analysed. Macroscopically, they appear spherical, with smooth edges and a compact, polished surface, although from the detail (Fig. 4—5B) it is possible to note the presence of a few small pores caused by the sudden loss of water during the freeze-drying process. The spherical, homogeneous structure and softness of the prepared microcapsules is an advantage, overcoming the problems of perception of roughness and grainy sensation in the mouth typical of multiparticulates can be an obstacle to patient acceptability (Kimura et al., 2015; Lopez et al., 2018, 2016).

The cross-section of the F_{s18} microcapsules shows a more homogeneous microstructure than the previous ones, much more like a matrix formulation. However, the core appears less dense than the shell, the structure is well organised and like a capillary structure. These internal structures, characterised by the presence of pores and channels (Fig. 4-5D), make the microcapsules float in water.

Floating formulations are advantageous to prolong the retention time of the dosage form in the stomach (El-Kamel et al., 2001). A formulation can be defined as floating in the stomach if its density is lower than that of gastric fluids. A multiparticulate floating system has advantages over a single-unit preparation because, with each subsequent gastric emptying, the sunken microcapsules distribute more evenly over a wide area of absorption sites, increasing the opportunity for a predictable drug release profile and absorption (Açikgöz et al., 1995).

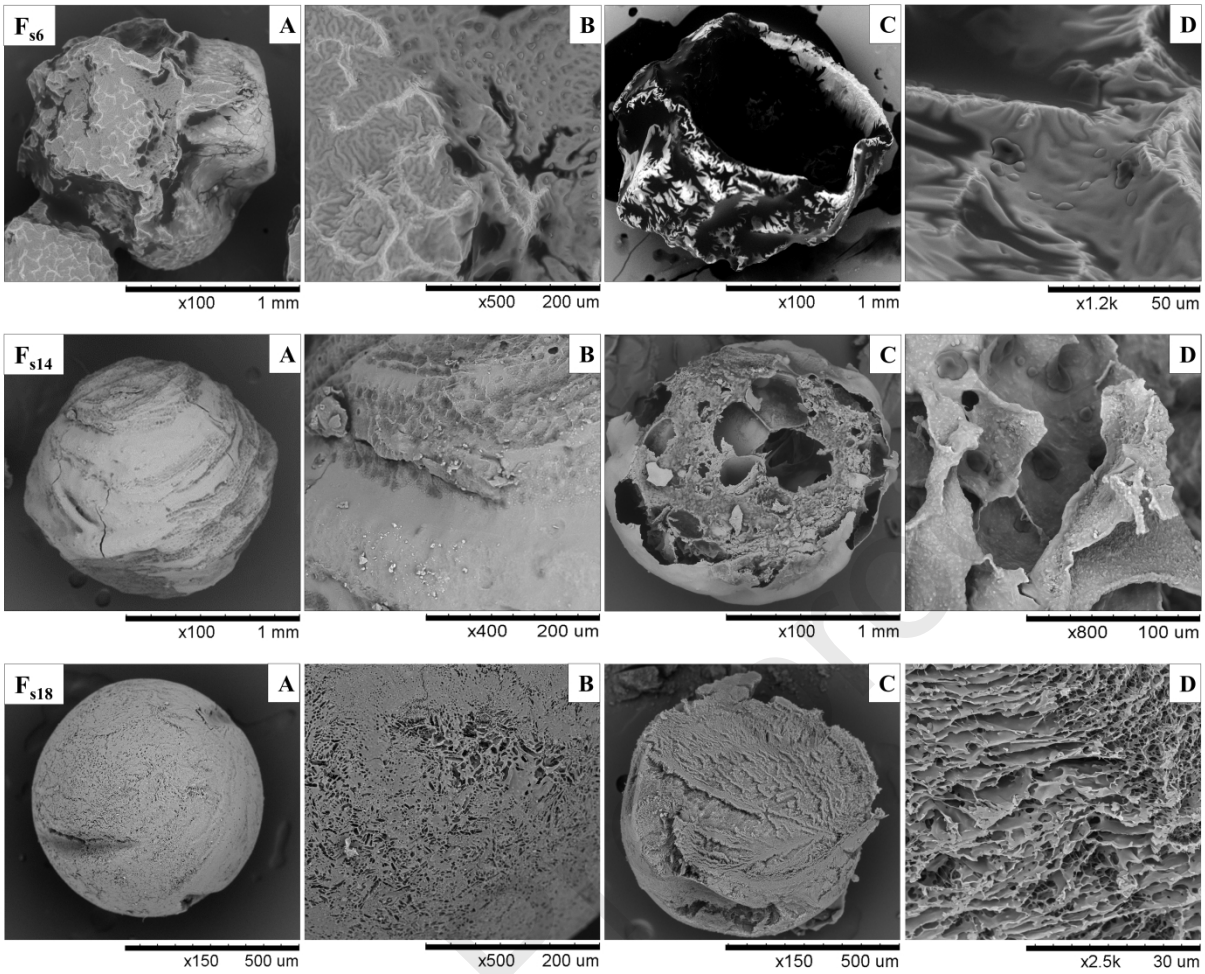

Fig. 4 5. SEM images of F_{s6}, F_{s14} and F_{s18} (A), their surface (B) and cross-sections (C and D).

3.7 Swelling behaviour

Swelling behaviours of the microcapsules were carried out to evaluate shell swelling in media with different pH values and to predictively evaluate the drug release behaviour of the microcapsules (Colombo, 1993). The results of the swelling study are shown in Fig. 6. For the F_{s6} and F_{s14} formulations, the study was conducted for 2 hours at pH 1.2 and then at pH 6.8. In contrast, for the F_{s18} formulations, the swelling study was only evaluated at pH 1.2 because, at the end of 2 hours, there were no more microcapsules in the basket. The F_{s14} microcapsules, as shown in Fig. ~~5a~~ 6A, increased their weight by 4.3 times at pH 1.2. Chitosan, thanks to its antacid and anti-ulcer characteristics, prevents or attenuates the irritation of drugs in the stomach and for this reason, it has been widely used for the sustained administration of drugs (How et al., 1985). Chitosan exhibits a pH-sensitive behaviour being a weak base, due to many amino groups in its chain (Fig. 1). From the observation of the graph, it is evident that the character of the swelling curves changes significantly over time at pH 1.2 compared to that at pH 6.8. At pH 1.2 the swelling reaches a stable equilibrium much more rapidly than at pH 6.8 where the swelling curve does not change much with time. After an initial substantial microcapsule swelling, it remained constant at pH 1.2 which could indicate that the dissolution tendency of the microcapsules exceeds the degree of swelling (Gupta and Kumar, 2000). Although after the swellings at pH 1.2, the microcapsules were swollen but still intact, oil droplets were clearly visible in the external medium.

The swelling behaviour of F_{s6} microcapsules is different (Fig. ~~5~~ 6A). Dry alginate/carbopol microcapsules increase their volume due to matrix rehydration and in accordance with the degree

of cross-linking with calcium (Bajpai and Sharma, 2004). The swelling process requires the initial transport of water and Na^+ ions into the microcapsules through the diffusion mechanism, followed by disintegration and erosion of the alginate microcapsules gel. The swelling of the microcapsules at 2 hours at pH 1.2 is 2.2 times their initial weight as the alginate in acid solutions hydrates and transforms into a porous and insoluble layer. However, the presence of carbopol has determined the appearance in the shell of a more porous structure with the consequent premature release of the encapsulated oil, clearly visible, already in the gastric environment. At higher pH values, such as those present in the intestinal tract (pH 6.8), the alginate transforms into a viscous and soluble layer with the consequent rapid dissolution of the alginate matrices which in this case takes place around 4 total hours of study with consequent disintegration of the microcapsules.

The F_{s18} microcapsules (Fig. ~~5~~ 6B) have a very different swelling profile from the other two. In fact, the study showed a rapid swelling reached at 15 minutes, with subsequent disintegration of the microcapsules. For this reason, the test was conducted only in an acid environment as at the end of the 2 hours the microcapsules were completely swelled and disintegrated.

The study suggested that all microcapsules made could be considered suitable for gastric delivery. The F_{s6} and F_{s14} microcapsules, even if they do not disintegrate at pH 1.2, can be considered suitable for a gastric delivery of the MIS as is clearly visible the oil in the external medium. MIS release from the core is controlled more by shell porosity than shell swelling or dissolution. Instead, in the case of the F_{s18} formulations they completely disintegrate at pH 1.2, as demonstrated by the swelling study, suggesting a complete and specific release of the MIS at the gastric level.

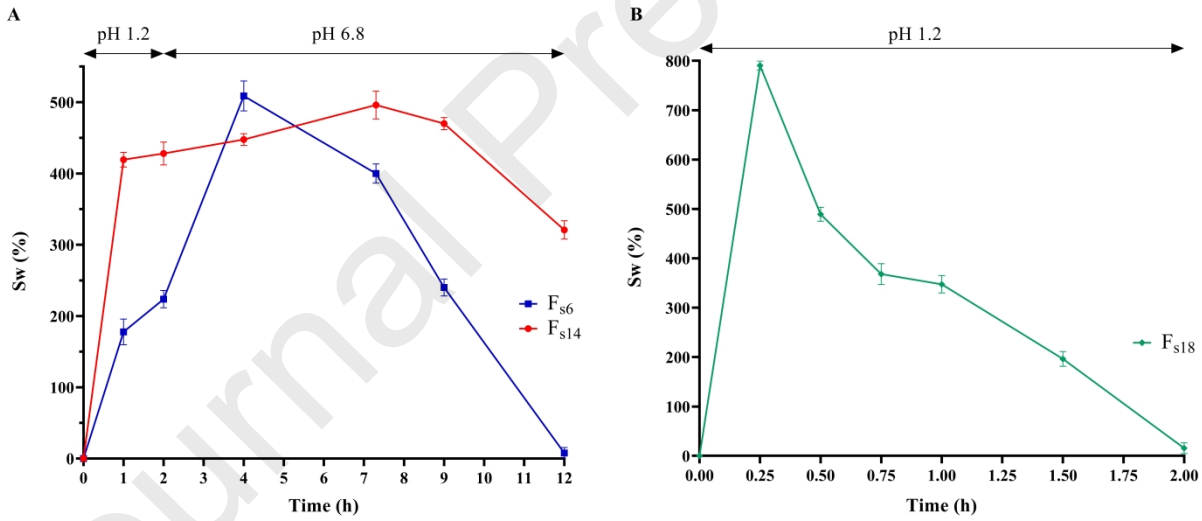

Fig. ~~5~~ 6. (A) Swelling profiles of microcapsules (F_{s6}-F_{s14}) at pH 1.2 and pH 6.8. (B) Swelling profile of microcapsules (F_{s18}) at pH 1.2.

3.8 Drug release

Release studies were conducted to confirm the ability of formulations to release MIS specifically and completely in the stomach. They supplied important information on the different properties and characteristics of the microcapsules produced that may influence the rate of drug release from them. Analyses in a simulated gastric environment at pH 1.2 provided details on the rate and pattern of drug release from the systems once it reached the stomach. In detail, Fig. ~~6~~ 7 shows the release profile of intact MIS in bulk fluid from the three selected formulations.

The F_{s6} and F_{s14} formulations resulted in immediate release of MIS; in fact, through a release study performed by direct method, after 5 minutes the F_{s6} formulation had released 89.32% and the F_{s14} 70.79% of MIS. Such rapid drug release was confirmed by the immediate release of oil

from the systems, which constitutes both the core of the formulations but also the vehicle in which MIS is present, which was clearly visible floating on the surface. This result can be attributed to the porous structure of the shell which favours the escape of the oil phase and the drug into the external gastric medium.

Although MIS has a Log P= 3.6, and thus a greater affinity to distribute in the oil phase than in the aqueous phase, the actual ratio of the oil phase to the aqueous phase being largely in favour of the aqueous phase, it can be assumed that the drug distributes more in the aqueous phase. To confirm the release data obtained at 5 minutes from both formulations, an evaluation by indirect method was performed to confirm the residual amount of MIS at 5 minutes in the microcapsules. Indeed, the absence of the drug after 5 minutes was evidenced in the F_{s6} microcapsules. The release study showed that as time increases, there is a decrease in the concentration of MIS in the aqueous phase. This is an expected result due to its chemical instability in the gastric environment as demonstrated by our kinetic degradation study (Supplementary Information, Fig. S~~1~~2) of the previous drug alone conducted at pH 1.2 at 37 °C. In contrast, the F_{s18} formulations showed a more gradual release in the first few minutes with a complete release in 30 min ~~in contrast~~ compared to the F_{s6} and F_{s14} formulations which showed a decrease in MIS concentration of 40.64% and 41.19% in 30 min and about 70% in 70 min respectively confirming the instability of the drug which was further proven by a mass study (Fig. S~~2~~3A). The release data obtained at 30 min for the F_{s18} formulation are significantly different ($p< 0.0001$) from the release values obtained by direct method from the F_{s6} and F_{s14} formulations. The MIS concentration in the F_{s18} formulation remained constant at 100% for the 70 min demonstrating the greater stability of MIS complexed with HP-β-CD in contrast to the F_{s6} and F_{s14} formulations where at 70 min there is 70% degradation of the drug. The greater stability in the gastric environment of the complexed drug was demonstrated by both HPLC analysis and LC-mass studies as shown in Figure S~~2~~3B in the Supplementary Information. In addition, the increased stability of ~~the product~~ MIS is related to several advantages including reduced dosage with enhanced reduction of side effects.

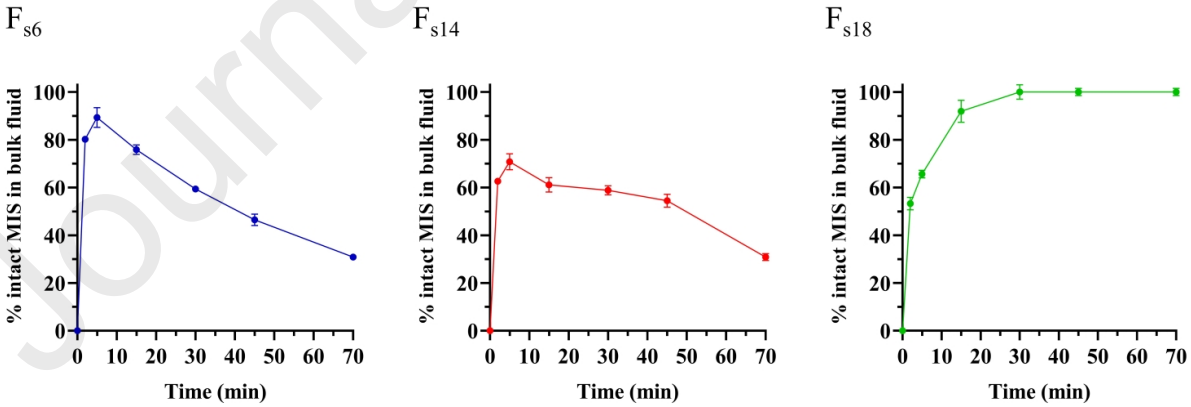

Fig. ~~6~~ 7. Drug release profile of F_{s6}, F_{s14} and F_{s18} in simulated gastric fluids at pH 1.2.

3.9 MIS Degradation Kinetic Study in Simulated Gastric Environment

The study of MIS degradation kinetics was performed to assess its chemical stability in the gastric environment with or without HP-β-CD. The decrease of the peak area of MIS and the appearance of degradation products were observed for the drug alone in the medium. After

plotting the three mathematical models, the results of the study agreed with a previous work (Monkhouse et al., 1973), showing first-order degradation kinetics described by Equation 14:

$$[A]_t = [A]_0 \times e^{-kt} \qquad (14)$$

Half-life, on the other hand, was calculated as $t_{1/2} = \frac{\ln 2}{k}$. The mean values of rate constant for MIS and its half-life were k = 0.00784 min^{-1} and 38.39 min respectively.

As the chemical instability of MIS is well known (Collins et al., 1985; Gu et al., 2005), a LC-Mass study of MIS and MIS/HP-β-CD in an acidic environment was performed in addition to the kinetic study of degradation. The samples were evaluated at time zero (t_0) and after 70 min (t_{70}) in a simulated gastric fluid at pH 1.2 and at 37°C. The mass spectrum of MIS (Fig. S3A) shows the typical peak m/z: 405.26 at t_0 while it disappears after 70 min. In parallel, the same experiment was performed with the MIS/HP-β-CD inclusion complex (Fig. S3B). The bell-shaped signals are typical of HP-β-CD and are due to the degree of cyclodextrin substitution (Laquintana et al., 2019). In contrast, the MIS peak remains unchanged at both t_0 and t_{70} min, confirming the protection of cyclodextrin against MIS and its greater stability at pH 1.2.

3.10 Physical Stability of Microcapsules and Chemical Stability of MIS in the Formulations

Stability studies were conducted under different storage conditions for F_{s6}, F_{s14} and F_{s18} microcapsules. The results obtained after 2 months for the F_{s18} formulations, irrespective of temperature, reveal that the drug and microcapsules are chemically and physically stable (visual and diameter analysis), respectively. The concentration of MIS examined by HPLC analysis in the microcapsules, under all conditions examined, remains constant (Table 6), despite the slight reduction in concentration at 40 °C. The F_{s18} formulation does not show any dimensional changes in the microcapsules and visual analysis did not reveal any colour changes on the surface, stickiness, or deterioration.

Although F_{s6} and F_{s14} show no dimensional or colour changes on the surface, a decrease in MIS concentration over time is observed with the appearance of degradation peaks in the HPLC chromatogram. F_{s6}, regardless of the way they were stored, showed stickiness due to the loss of oil from the core. The MIS concentration at 2 months is drastically reduced when the microcapsules are stored at 25 °C and 40 °C due to both the chemical instability of MIS and its loss to the surface of the microcapsules. However, this figure is quite different from that obtained for the F_{s18} formulations stored for two months at 40 °C, which maintained good stability (87.28%) of MIS due to the presence of cyclodextrin, which exerts its stabilising (Ghodke et al., 2010; Kali et al., 2024) and protective action against MIS.

Table 6. EE% in the microcapsules at time zero (t_0), and 2 months (t_2) in different conditions. Data are reported as the mean of results ± SD.

Formulation Code	EE% ($t_{0\ months}$)	EE% ($t_{2\ months\ at\ 4\ °C}$)	EE% ($t_{2\ months\ at\ 25\ °C}$)	EE% ($t_{2\ months\ at\ 40\ °C}$)
F_{s6}	59.86 ± 6.85	5.13 ± 0.37	3.88 ± 0.28	-
F_{s14}	69.99 ± 5.13	46.08 ± 3.58	47.03 ± 3.66	-
F_{s18}	97.61 ± 4.15	97.24 ± 0.16	96.17 ± 1.84	87.28 ± 3.07

4 Conclusion

The present research investigated the prilling/vibration technique to encapsulate MIS in microcapsules for site-specific gastric delivery. Different feeds that would form the shell of the microcapsules were prepared to identify those most suitable for the prilling technique. The processing parameters were studied, and the most suitable ones were selected to process the prepared feeds. In particular, the most promising formulations (F_{s6}, F_{s14}, and F_{s18}) were chosen from 18 possibilities. The drug was then loaded into these formulations in their original form (F_{s6} and F_{s14}) with an oil core or as an inclusion complex (F_{s18}). Microcapsules were created to encapsulate MIS, with the aim of gastric delivery and increased stability. The prilling/vibration technique produces more flexible formulations in terms of dosage, where the increased stability of MIS could reduce dosage with a potential reduction in side effects. The microcapsules produced were analysed for size, yield, encapsulation efficiency, swelling, and release studies. The results demonstrate that these systems are suitable for oral administration in different population groups due to their diameters, dosing flexibility and promising flow properties. Among the three formulations, ~~F_{s16}~~ F_{s18} exhibited gastric release within 30 minutes and proved to be the most suitable formulation because the presence of the MIS/HP-β-CD inclusion complex ensured a greater ability to stabilise MIS in the simulated gastric environment.
In conclusion, these microcapsules, produced using the prilling/vibration technique, present a robust and reliable approach to both increasing the chemical stability of MIS and allowing its release in the stomach, representing a possible alternative approach to commercially available drugs.

Declaration of Competing Interest
The authors declare that they have no known competing financial interests or personal relationships that could have appeared to influence the work reported in this paper.

Data availability
The datasets generated during and/or analysed during the current study are available from the corresponding author on reasonable request.

Acknowledgements
Authors thank Mr. Nicola Di Masi (Department of Pharmacy-Pharmaceutical Sciences UNIBA) for his skilful technical assistance in recording NMR spectra and Mr. Pasquale Trotti (DISSPA UNIBA) for his contribution to SEM analysis.

Author contributions
Vita D'Amico: Methodology, Investigation, Writing—original draft. Nunzio Denora: Conceptualization, Supervision, Funding acquisition. Marianna Ivone: Methodology, Acquisition of data. Rosa Maria Iacobazzi: Writing—review & editing, Validation. Valentino Laquintana: Data analysis, Software. Annalisa Cutrignelli: Methodology, Interpretation of data. Massimo Franco: Supervision, Data curation. Michele Barone: Writing—review & editing, Resources. Antonio Lopalco: Conceptualization and design of the work, Methodology, Writing—original draft, Supervision. Angela Assunta Lopedota: Conceptualization and design of the work, Methodology, Writing—review & editing, Supervision.

Funding
This research received no external founding from agencies in the public, commercial or not-for-profit sectors.

References

Abdullah, E.C., Geldart, D., 1999. The use of bulk density measurements as flowability indicators. Powder Technol 102, 151–165. https://doi.org/https://doi.org/10.1016/S0032-5910(98)00208-3

Açikgöz, M., Kaş, H.S., Hasçelik, Z., Milli, U., Hincal, A.A., 1995. Chitosan microspheres of diclofenac sodium, II: In vitro and in vivo evaluation. Pharmazie 40, 275–277.

Adebisi, A., Conway, B.R., 2011. Gastroretentive microparticles for drug delivery applications. J Microencapsul 28, 689–708. https://doi.org/10.3109/02652048.2011.590613

Aquino, R.P., Auriemma, G., D'Amore, M., D'Ursi, A.M., Mencherini, T., Del Gaudio, P., 2012. Piroxicam loaded alginate beads obtained by prilling/microwave tandem technique: Morphology and drug release. Carbohydr Polym 89, 740–748. https://doi.org/doi:10.1016/j.carbpol.2012.04.003

Bajpai, S.K., Sharma, S., 2004. Investigation of swelling/degradation behaviour of alginate beads crosslinked with Ca2+ and Ba2+ ions. React Funct Polym 59, 129–140. https://doi.org/10.1016/j.reactfunctpolym.2004.01.002

Bellad, M.B., Goudar, S.S., 2006. Misoprostol: Theory and Practice, in: Arulkumaran Karoshi, Keith Lalonde, B-Lynch (Eds.), A Textbook of Postpartum Haemorrhage. Duncowt. Duncow, UK, pp. 114–126.

Bera, K., Mazumder, B., Khanam, J., 2016. Study of the Mucoadhesive Potential of Carbopol Polymer in the Preparation of Microbeads Containing the Antidiabetic Drug Glipizide. AAPS PharmSciTech 17, 743–756. https://doi.org/10.1208/s12249-015-0396-8

Berard, V., Fiala, C., Cameron, S., Bombas, T., Parachini, M., Gemzell-Danielsson, K., 2014. Instability of Misoprostol Tablets Stored Outside the Blister: A Potential Serious Concern for Clinical Outcome in Medical Abortion. PLoS One 9, e112401. https://doi.org/10.1371/journal.pone.0112401

Bhangare, D., Rajput, N., Jadav, T., Sahu, A.K., Tekade, R.K., Sengupta, P., 2022. Systematic strategies for degradation kinetic study of pharmaceuticals: an issue of utmost importance concerning current stability analysis practices. J Anal Sci Technol 13. https://doi.org/doi.org/10.1186/s40543-022-00317-6

Bimrew Sendekie Belay, 1990. Stabilization of misoprostol with hydroxypropyl methylcellulose (HPMC) against degradation by water. Pharmaceutical Research 7, 1186–1189. https://doi.org/doi:10.1023/a:1015996712794

Bizimana, T., Hagen, N., Gnegel, G., Kayumba, P.C., Heide, L., 2021. Quality of oxytocin and misoprostol in health facilities of Rwanda. PLoS One 16, e0245054. https://doi.org/doi: 10.1371/journal.pone.0245054

Bonacucina, G., Di Martino, P., Piombetti, M., Colombo, A., Roversi, F., Palmieri, G.F., 2006. Effect of plasticizers on properties of pregelatinised starch acetate (Amprac 01) free films. Int J Pharm 313, 72–77. https://doi.org/10.1016/j.ijpharm.2006.01.046

Breitkreutz, J., Boos, J., 2007. Paediatric and geriatric drug delivery. Expert Opin Drug Deliv 4, 37–45. https://doi.org/10.1517/17425247.4.1.37

Brewster, M.E., Loftsson, T., 2007. Cyclodextrins as pharmaceutical solubilizers. Adv Drug Deliv Rev 59, 645–666. https://doi.org/10.1016/j.addr.2007.05.012

Collins, P.W., Pappo, R., Dajani, E.Z., 1985. Chemistry and Synthetic Development of Misoprostol. Digestive diseases and sciencesestive Diseases and Sciences 30, 114S-117S. https://doi.org/doi.org/10.1007/BF01309395

Colombo, P., 1993. Swelling-controlled release in hydrogel matrices for oral route. Adv Drug Deliv Rev 11, 37–57. https://doi.org/10.1016/0169-409X(93)90026-Z

D'Amico, V., Arduino, I., Vacca, M., Maria, R., Altamura, D., Lopalco, A., Rizzi, R., Cutrignelli, A., Laquintana, V., Massimo, F., Angelis, M. De, Denora, N., Assunta, A., 2023. Colonic budesonide delivery by multistimuli alginate / Eudragit ® FS 30D / inulin-based microspheres as a paediatric formulation. Carbohydr Polym 302, 120422. https://doi.org/10.1016/j.carbpol.2022.120422

D'Aria, F., Pagano, B., Giancola, C., 2022. Thermodynamic properties of hydroxypropyl-β-cyclodextrin/guest interaction: a survey of recent studies. J Therm Anal Calorim 147, 4889–4897. https://doi.org/10.1007/s10973-021-10958-1

Del Gaudio, P., Colombo, P., Colombo, G., Russo, P., Sonvico, F., 2005. Mechanisms of formation and disintegration of alginate beads obtained by prilling. Int J Pharm 302, 1–9. https://doi.org/10.1016/j.ijpharm.2005.05.041

Del Gaudio, P., Russo, P., Rosaria Lauro, M., Colombo, P., Aquino, R.P., 2009. Encapsulation of ketoprofen and ketoprofen lysinate by prilling for controlled drug release. AAPS PharmSciTech 10, 1178–1185. https://doi.org/10.1208/s12249-009-9309-z

El-Kamel, A., Sokar, M., Al Gamal, S., Naggar, V., 2001. Preparation and evaluation of ketoprofen floating oral delivery system 1. Int J Pharm 220, 13–21. https://doi.org/https://doi.org/10.1016/S0378-5173(01)00574-9

Garris, R.E., Kirkwood, C.F., 1989. Misoprostol: a prostaglandin E1 analogue. Clin Pharm 8, 627–44.

Ghodke, D., Ghodke, G., Patil, K., Nakhat, PD, Nakhat, PG, Naikwade, N., Magdum, C., 2010. Solid state characterization of domperidone: Hydroxypropyl-b-cyclodextrin inclusion complex. Indian J Pharm Sci 72, 245. https://doi.org/10.4103/0250-474X.65032

Gould, S., Scott, R.C., 2005. 2-Hydroxypropyl-β-cyclodextrin (HP-β-CD): A toxicology review. Food and Chemical Toxicology 43, 1451–1459. https://doi.org/10.1016/j.fct.2005.03.007

Gu, F., Cui, F., Gao, Y., 2005. Preparation of prostaglandin E1-hydroxypropyl-β-cyclodextrin complex and its nasal delivery in rats. Int J Pharm 290, 101–108. https://doi.org/10.1016/j.ijpharm.2004.11.021

Gupta, K.C., Kumar, M.N.V.R., 2000. Drug release behavior of beads and microgranules of chitosan. Biomaterials 21, 1115–1119. https://doi.org/https://doi.org/10.1016/S0142-9612(99)00263-X.

Hagen, N., Bizimana, T., Kayumba, P.C., Khuluza, F., Heide, L., 2020. Stability of misoprostol tablets collected in Malawi and Rwanda: Importance of intact primary packaging. PLoS One 15, e0238628. https://doi.org/doi: 10.1371/journal.pone.0238628

Higuchi T., Connors K. A., 1965. Phase solubility techniques. Advanced Analytical Chemistry of Instrumentation 4, 117–212.

How, W.M., Miyazaki, S., Takada, M., Komai, T., 1985. Sustained release of indomethacin from chitosan granules. Chem Pharm Bull (Tokyo) 33, 3986–3992. https://doi.org/doi:10.1248/cpb.33.3986

Ist. Poligrafo dello Stato, 2008. Italian Official Pharmacopoeia. pp. 417–423.

Jadach, B., Świetlik, W., Froelich, A., 2022. Sodium Alginate as a Pharmaceutical Excipient: Novel Applications of a Well-known Polymer. J Pharm Sci 111, 1250–1261. https://doi.org/10.1016/j.xphs.2021.12.024

Jyothi, N.V.N., Prasanna, P.M., Sakarkar, S.N., Prabha, K.S., Ramaiah, P.S., Srawan, G.Y., 2010. Microencapsulation techniques, factors influencing encapsulation efficiency. J Microencapsul 27, 187–197. https://doi.org/10.3109/02652040903131301

Kahsay, G., Song, H., Eerdekens, F., Tie, Y., Hendriks, D., Van Schepdael, A., Cabooter, D., Adams, E., 2015. Development and validation of LC methods for the separation of misoprostol related substances and diastereoisomers. J Pharm Biomed Anal 111, 91–99. https://doi.org/https://doi.org/10.1016/j.jpba.2015.03.028.

Kali, G., Haddadzadegan, S., Bernkop-Schnürch, A., 2024. Cyclodextrins and derivatives in drug delivery: New developments, relevant clinical trials, and advanced products. Carbohydr Polym 324. https://doi.org/10.1016/j.carbpol.2023.121500

Kankate, D., Panpalia, S.G., Kumar, K.J., Kennedy, J.F., 2020. Studies to predict the effect of pregelatinization on excipient property of maize and potato starch blends. Int J Biol Macromol 164, 1206–1214. https://doi.org/10.1016/j.ijbiomac.2020.07.170

Kararli, T.T., Catalano, T., Needham, T.E., Finnegan, P.M., Searle, G.D., 1991. Mechanism of misoprostol stabilization in hydroxypropyl methylcellulose. Adv Exp Med Biol 302, 275–289. https://doi.org/doi:10.1007/978-1-4899-0664-9_15

Khan, D., Kirby, D., Bryson, S., Shah, M., Rahman Mohammed, A., 2022. Paediatric specific dosage forms: Patient and formulation considerations. Int J Pharm 616. https://doi.org/10.1016/j.ijpharm.2022.121501

Kimura, S.I., Uchida, S., Kanada, K., Namiki, N., 2015. Effect of granule properties on rough mouth feel and palatability of orally disintegrating tablets. Int J Pharm 484, 156–162. https://doi.org/10.1016/j.ijpharm.2015.02.023

Laquintana, V., Asim, M.H., Lopedota, A., Cutrignelli, A., Lopalco, A., Franco, M., Bernkop-Schnürch, A., Denora, N., 2019. Thiolated hydroxypropyl-β-cyclodextrin as mucoadhesive excipient for oral delivery of budesonide in liquid paediatric formulation. Int J Pharm 572, 118820. https://doi.org/doi:10.1016/j.ijpharm.2019.118820

Loftsson, T., Hreinsdóttir, D., Másson, M., 2005. Evaluation of cyclodextrin solubilization of drugs. Int J Pharm 302, 18–28. https://doi.org/10.1016/j.ijpharm.2005.05.042

Lopalco, A., Denora, N., Laquintana, V., Cutrignelli, A., Franco, M., Robota, M., Hauschildt, N., Mondelli, F., Arduino, I., Lopedota, A., 2020. Taste masking of propranolol hydrochloride by microbeads of EUDRAGIT® E PO obtained with prilling technique for paediatric oral administration. Int J Pharm 574, 118922. https://doi.org/10.1016/j.ijpharm.2019.118922

Lopalco, A., Manni, A., Keeley, A., Haider, S., Li, W., Lopedota, A., Altomare, C.D., Denora, N., Tuleu, C., 2022. In Vivo Investigation of (2-Hydroxypropyl)-β-cyclodextrin-Based Formulation of Spironolactone in Aqueous Solution for Paediatric Use. Pharmaceutics 14, 780. https://doi.org/10.3390/pharmaceutics14040780

Lopedota, A., Cutrignelli, A., Laquintana, V., Franco, M., Donelli, D., Ragni, L., Tongiani, S., Denora, N., 2015. β-cyclodextrin in personal care formulations: role on the complexation of malodours causing molecules. Int J Cosmet Sci 37, 438–445. https://doi.org/10.1111/ics.12215

Lopedota, A.A., Arduino, I., Lopalco, A., Iacobazzi, R.M., Cutrignelli, A., Laquintana, V., Racaniello, G.F., Franco, M., la Forgia, F., Fontana, S., Denora, N., 2021. From oil to microparticulate by prilling technique: Production of polynucleate alginate beads loading Serenoa Repens oil as intestinal delivery systems. Int J Pharm 599, 120412. https://doi.org/10.1016/j.ijpharm.2021.120412

Lopez, F.L., Bowles, A., Gul, M.O., Clapham, D., Ernest, T.B., Tuleu, C., 2016. Effect of formulation variables on oral grittiness and preferences of multiparticulate formulations in adult volunteers. European Journal of Pharmaceutical Sciences 92, 156–162. https://doi.org/10.1016/j.ejps.2016.07.006

Lopez, F.L., Ernest, T.B., Tuleu, C., Gul, M.O., 2015. Formulation approaches to pediatric oral drug delivery: Benefits and limitations of current platforms. Expert Opin Drug Deliv 12, 1727–1740. https://doi.org/10.1517/17425247.2015.1060218

Lopez, F.L., Mistry, P., Batchelor, H.K., Bennett, J., Coupe, A., Ernest, T.B., Orlu, M., Tuleu, C., 2018. Acceptability of placebo multiparticulate formulations in children and adults. Sci Rep 8. https://doi.org/10.1038/s41598-018-27446-6

Mahmood, A., Bonengel, S., Laffleur, F., Ijaz, M., Leonaviciute, G., Bernkop-Schnürch, A., 2015. An in-vitro exploration of permeation enhancement by novel polysulfonate thiomers. Int J Pharm 496, 304–313. https://doi.org/10.1016/j.ijpharm.2015.10.013

Monkhouse, D.C., van Campen, L., Aguiar, A.J., 1973. Kinetics of Dehydration and Isomerization of Prostaglandins E1 and E2. J Pharm Sci 62, 576–580. https://doi.org/10.1002/jps.2600620406

Odabasoglu, F., Halici, Z., Cakir, A., Halici, M., Aygun, H., Suleyman, H., Cadirci, E., Atalay, F., 2008. Beneficial effects of vegetable oils (corn, olive and sunflower oils) and α-tocopherol on anti-inflammatory and gastrointestinal profiles of indomethacin in rats. Eur J Pharmacol 591, 300–306. https://doi.org/10.1016/j.ejphar.2008.06.075

Oth, M., Franz, M., Timmermans, J., Möes, A., 1992. The Bilayer Floating Capsule: A Stomach-Directed Drug Delivery System for Misoprostol. Pharmaceutical Research: An Official Journal of the American Association of Pharmaceutical Scientists 9, 298–302. https://doi.org/10.1023/A:1015870314340

Patel, J.A., Roseman, T.J., Sims, B., Stehle, R.G., 1973. Stability of Prostaglandins. American Journal of Health-System Pharmacy 30, 236–239. https://doi.org/10.1093/ajhp/30.3.236

Rough, S.L., Wilson, D.I., Bayly, A., York, D., 2003. Tapping characterisation of high shear mixer agglomerates made with ultra-high viscosity binders. Powder Technol 132, 249–266. https://doi.org/10.1016/S0032-5910(03)00075-5

Russo, E., Selmin, F., Baldassari, S., Gennari, C.G.M., Caviglioli, G., Cilurzo, F., Minghetti, P., Parodi, B., 2016. A focus on mucoadhesive polymers and their application in buccal dosage forms. J Drug Deliv Sci Technol 32, 113–125. https://doi.org/doi.org/10.1016/j.jddst.2015.06.016

Santos, E.H., Kamimura, J.A., Hill, L.E., Gomes, C.L., 2015. Characterization of carvacrol beta-cyclodextrin inclusion complexes as delivery systems for antibacterial and antioxidant applications. LWT - Food Science and Technology 60, 583–592. https://doi.org/10.1016/j.lwt.2014.08.046

Saokham, P., Muankaew, C., Jansook, P., Loftsson, T., 2018. Solubility of Cyclodextrins and Drug/Cyclodextrin Complexes. Molecules 23, 1161. https://doi.org/10.3390/molecules23051161

Sen, O., Manna, S., Nandi, G., Jana, Subrata, Jana, Sougata, 2023. Recent advances in alginate based gastroretentive technologies for drug delivery applications. Med Nov Technol Devices 18, 100236. https://doi.org/10.1016/j.medntd.2023.100236

Soppimath, K.S., Kulkarni, A.R., Aminabhavi, T.M., 2001. Development of hollow microspheres as floating controlled-release systems for cardiovascular drugs: Preparation and release characteristics. Drug Dev Ind Pharm 27, 507–515. https://doi.org/10.1081/DDC-100105175

Souza, M.P.C. de, Sábio, R.M., Ribeiro, T. de C., Santos, A.M. dos, Meneguin, A.B., Chorilli, M., 2020. Highlighting the impact of chitosan on the development of gastroretentive drug delivery systems. Int J Biol Macromol 159, 804–822. https://doi.org/10.1016/j.ijbiomac.2020.05.104

Tiwari, G., Tiwari, R., Rai, A., 2010. Cyclodextrins in delivery systems: Applications. J Pharm Bioallied Sci 2, 72. https://doi.org/10.4103/0975-7406.67003

Uyen, N.T.T., Hamid, Z.A.A., Tram, N.X.T., Ahmad, N., 2020. Fabrication of alginate microspheres for drug delivery: A review. Int J Biol Macromol 153, 1035–1046. https://doi.org/10.1016/j.ijbiomac.2019.10.233

Vega, E., Egea, Calpena, Espina, García, 2012. Role of hydroxypropyl-β-cyclodextrin on freeze-dried and gamma-irradiated PLGA and PLGA-PEG diblock copolymer nanospheres for ophthalmic flurbiprofen delivery. Int J Nanomedicine 7, 1357–1371. https://doi.org/10.2147/IJN.S28481

Walsh, J., Bickmann, D., Breitkreutz, J., Chariot-Goulet, M., 2011. Delivery devices for the administration of paediatric formulations: Overview of current practice, challenges and recent developments. Int J Pharm 415, 221–231. https://doi.org/10.1016/j.ijpharm.2011.05.048

Wlese, M., Cordes, H.-P., Chi, H., Seydel, J.K., Backensfeld, T., Muller, B.W., 1991. Interaction of Prostaglandin E1 with α-Cyclodextrin in Aqueous Systems: Stability of the Inclusion Complex. J Pharm Sci 80, 153–156. https://doi.org/doi:10.1002/jps.2600800213

Zaghloul, N., El Hoffy, N.M., Mahmoud, A.A., Elkasabgy, N.A., 2022. Cyclodextrin Stabilized Freeze-Dried Silica/Chitosan Nanoparticles for Improved Terconazole Ocular Bioavailability. Pharmaceutics 14, 470. https://doi.org/10.3390/pharmaceutics14030470

Zheng, Y., Liu, R., Hou, X., Zhuang, X., Wu, H., Yin, D., Yang, Y., 2023. Structural and physicochemical properties of microwave-processing pregelatinized maize starch, and its influence on drug release from tablets. J Drug Deliv Sci Technol 84, 104452. https://doi.org/10.1016/j.jddst.2023.104452

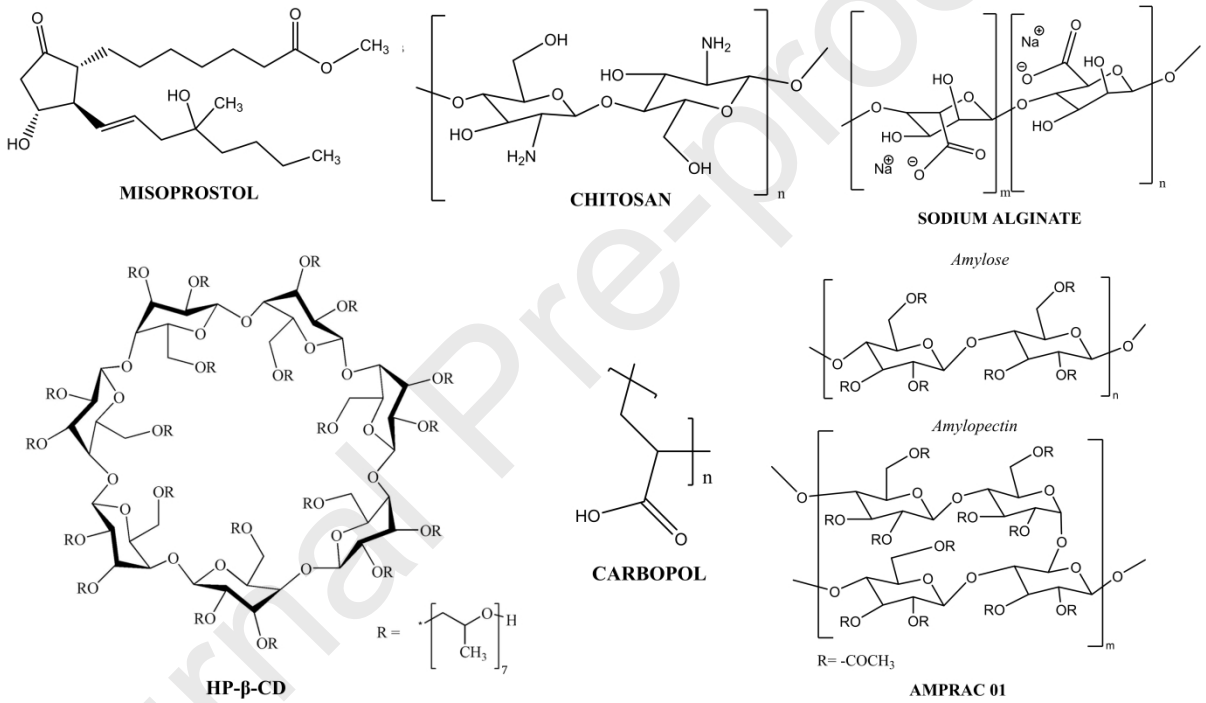

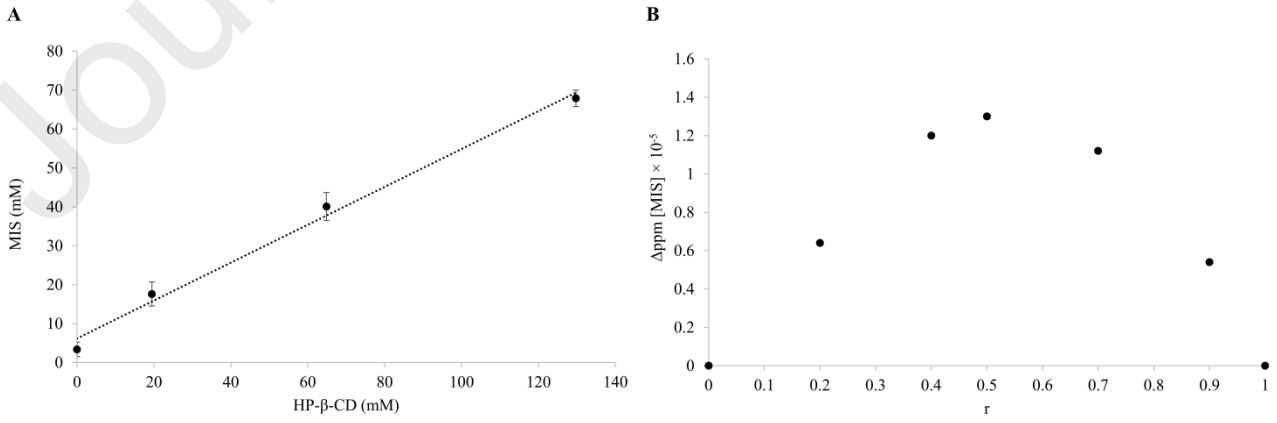

^{1}H-NMR

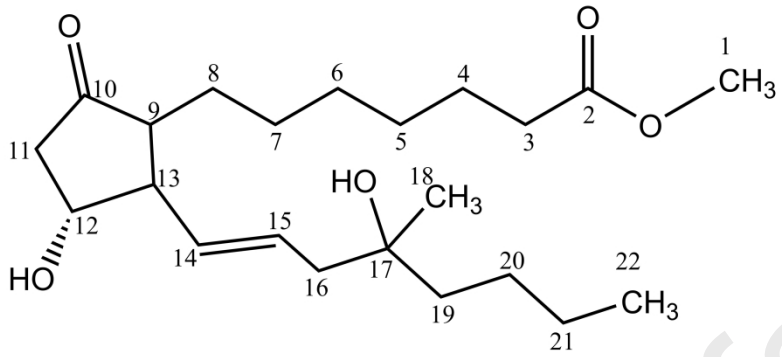

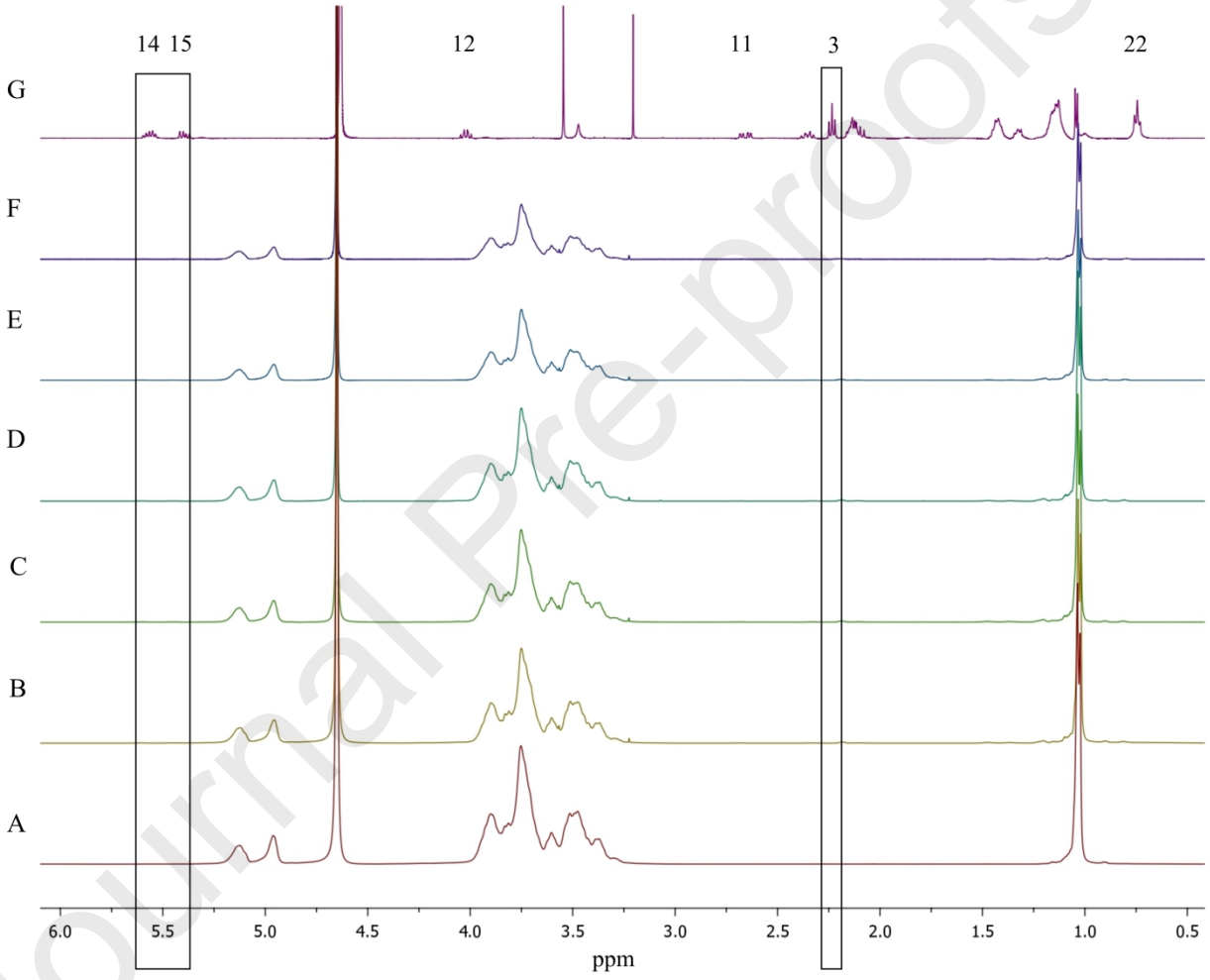

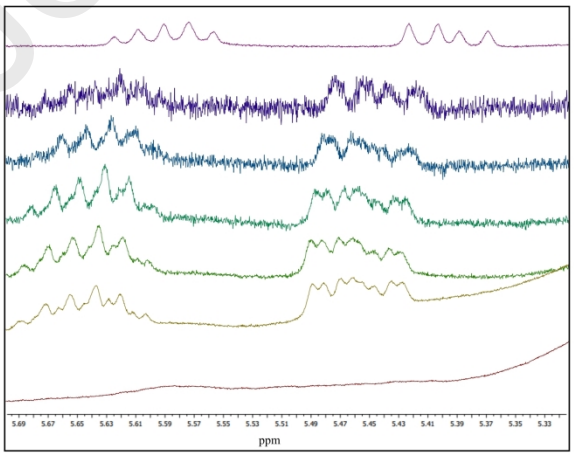

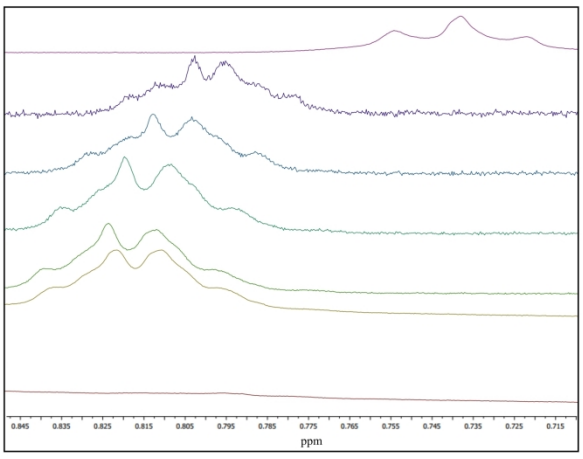

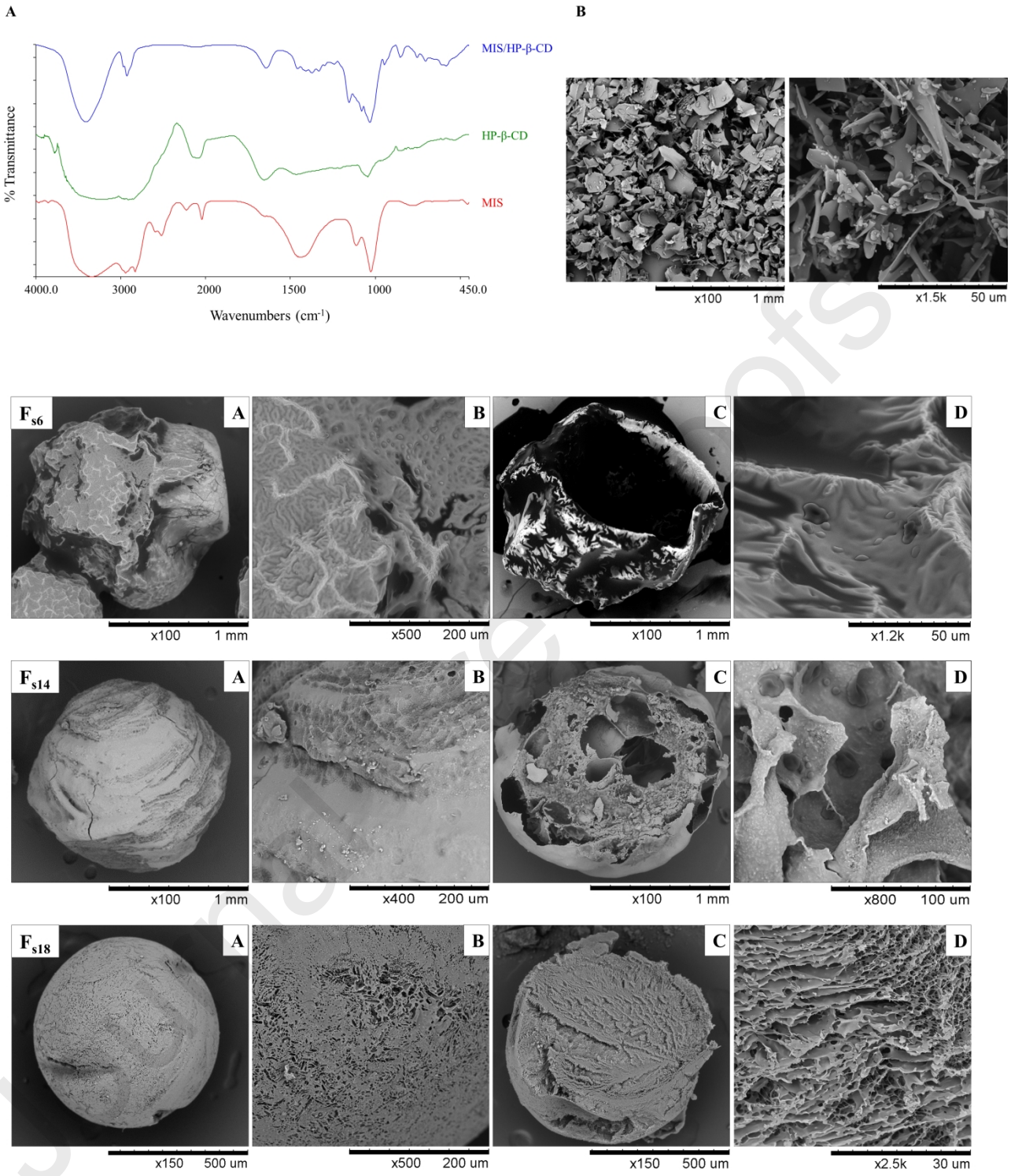
A
MIS/HP-β-CD
HP-β-CD
MIS
% Transmittance
4000.0
3000
2000
1500
1000
450.0
Wavenumbers (cm-1)
B
x100 1 mm
x1.5k 50 um
Fs6
A
x100 1 mm
B
x500 200 um
C
x100 1 mm
D
x1.2k 50 um
Fs14
A
x100 1 mm
B
x400 200 um
C
x100 1 mm
D
x800 100 um
Fs18
A
x150 500 um
B
x500 200 um
C
x150 500 um
D
x2.5k 30 um

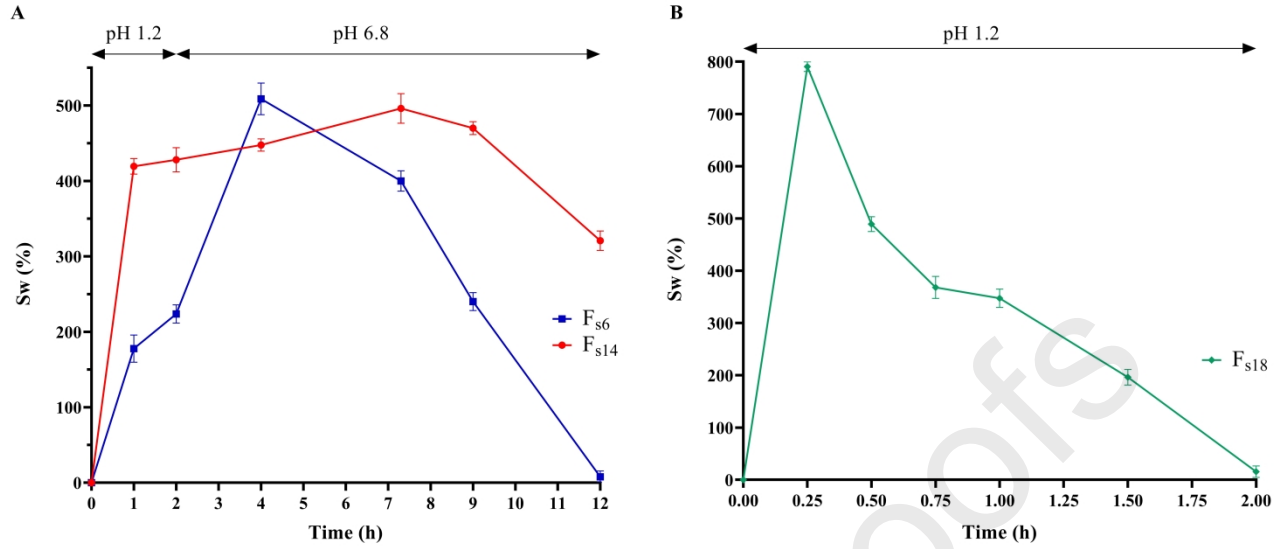

1035